Journal of Sound and Vibration 556 (2023) 117719

Contents lists available at ScienceDirect

Journal of Sound and Vibration

journal homepage: www.elsevier.com/locate/jsvi

Dynamic analysis of multi-cracked truss and frame structures with uncertain-but-bounded damage

Roberta Santoro [a,*], Cristina Gentilini [b]

[a] Department of Engineering, University of Messina, Villaggio S. Agata, Messina 98166, Italy
[b] Department of Architecture, University of Bologna, Viale del Risorgimento 2, Bologna 40136, Italy

ARTICLE INFO

Keywords:
Uncertain-but-bounded damage
Frame structure
Truss structure
Cracked member
Dynamic structural response
Open edge crack

ABSTRACT

The present paper aims to provide a contribution in the study of the dynamic response of cracked truss-like and frame-like structures with uncertain damage modeled by following a non-probabilistic approach. By adopting a finite element model to describe the cracked members with fully open cracks, in the framework of the interval analysis, the parameters identifying the cracks depths are modeled as uncertain-but-bounded variables.

The proposed procedure allows to evaluate lower and upper bounds of the time-varying response of multi-cracked trusses and frames subjected to deterministic excitation by applying two parallel generalized modal analyses corresponding to two appropriate combinations of the endpoints of the interval uncertainties. The method is validated through numerical tests and its accuracy is confirmed by the excellent agreement between the response bounds calculated via the present approach compared with the exact reference bounds derived by a combinatorial procedure (vertex method) merged with the Monte Carlo method.

1. Introduction

Most of the members of truss and frame structures can undergo to damages or cracks in overstressed zones due to several reasons. The presence of a crack in a structural member causes local changes in stiffness, whose entity mainly depends on the location and depth of the crack. These variations, in turn, have a significant effect on the dynamic behavior of the whole structure. The scientific research dealing with the study of the dynamic behavior of truss and frame structures with cracked elements can be roughly divided into three main groups depending on the hypotheses adopted on the extension and/or position of the damage: completely unknown, completely known and modeled as random variables. The principal aim of the former group is the identification of damage in terms of its position and extension through different dynamic techniques (natural frequency-based methods [1], mode shape-based methods, curvature/strain mode shape-based methods [2] and other methods based on modal parameters [3,4]).

The second group of methods considers to know exactly the position and/or severity of the damage in a structure and studies how the dynamic behavior changes in presence of damage. This topic has been extensively investigated in literature [5–15]. In these methods, the modeling of the damage in a member is a key aspect. Usually, the rotational spring model [7,15] or the simple reduction of stiffness [8] decreasing the cross-sectional area or the Young's modulus of the damaged element is adopted. Different models have been presented in literature proposing expressions of the spring stiffness equivalent to the crack for a large number of cases, concerning different geometry of the cross-section and different crack shapes. In Labib et al. [12], the free vibration of beams and frames with

* Corresponding author.
E-mail address: roberta.santoro@unime.it (R. Santoro).

https://doi.org/10.1016/j.jsv.2023.117719
Received 9 September 2022; Received in revised form 9 February 2023; Accepted 11 April 2023
Available online 12 April 2023

multiple single-edge cracks are studied modeling the crack as a rotational spring with stiffness depending on the crack depth. In Barad et al. [11], the problem of crack detection in a cantilever beam is solved modeling the edge crack as a rotational spring whose stiffness depends on the crack location and depth, while in [13] a study on axially loaded frames affected by multiple cracks is presented.

In the aforementioned approaches, the crack depth and position along the element of the structure are considered as deterministic quantities, i.e. depth and/or position of the damage are supposed to be known. However, in many structures these quantities are unknown and only a hypothesis on their values can be considered due the unavoidable uncertainty affecting the severity and position of the damage. In most of the existing studies involving damaged structures in presence of uncertain damage, the most common model used to describe the uncertain parameters characterizing the cracks is the probabilistic one according to which the uncertainty is defined as a random variable. This model assumes that sufficient experimental data is available in order to properly define an appropriate probability density function for the random variable [16]. Several studies have investigated the behavior of single- and multi-damaged beams with random cracks parameters in both static [17] and dynamic setting [18–23].

The probabilistic characterization of the static response of truss and frame structures with cracked members where the crack depth and location are assumed to as uniformly distributed random variables is carried out in Gentilini et al. [24,25].

However, data concerning the probability density functions of the damage are not always available and defined. For this case it is possible to rely on non-probabilistic models and in particular on interval analysis which represents a suitable alternative for uncertain problems with clear boundaries but with deficient data about probability distribution for the involved uncertainties. In the interval analysis based on the classical interval algebraic rules introduced firstly by Moore [26], an uncertain variable is represented by an interval of numbers, between a lower bound (LB) and an upper bound (UB), which presumably contains the unknown exact value of the variable under study and for this reason labelled also as uncertain-but-bounded variable.

In many structural problems in presence of uncertain-but-bounded parameters, several interval analysis methods have been proposed. In Kulpa et al. [27], the potentialities of application of interval methods for the analysis of linear mechanical systems with uncertain parameters is presented. In particular, the stiffness and the length of member in a structure are considered uncertain, hence modelled as interval numbers. In Wei et al. [28], the static response analysis of uncertain structures with unknown but bonded parameters is presented and in Ma and Li [29], a beam, a 3D truss, and a truck frame are considered to illustrate the accuracy and efficiency of the method. Aiming to reduce the overestimation (the so-called dependency phenomenon [30,31]) in the interval response due to the application of the classical interval analysis, several interval methods have been introduced in the finite element context [31] and applied to solve problems with interval coefficients in static and dynamic setting. Among these methods we mention e.g. the Taylor series expansion [32,33], the interval perturbation method [34,35], the Chebyshev interval expansion [36], the iterative approach [37] and the Interval Rational Series Expansion [38–40].

In the framework of cracked structures not many papers deal with the modeling of uncertain crack parameters via interval approach. The interval static response of multi-cracked beams in the most general case of simultaneous uncertainty in the size and position of the cracks has been evaluated in Santoro et al. [41] and an extensive comparative analysis on multi-damaged beams has been conducted in [42] where the parameters characterizing the cracks are modelled as random variables as well as uncertain-but-bounded parameters. In the frequency domain, the interval response of single and multi-cracked beams has been examined in [22,23,43] considering the uncertainty in the amplitude of the crack and resorting to a properly modified finite element centered around the crack; the frequency response of multi-cracked beams treated by the classical continuous beam equations with the generic crack represented by a massless rotational spring has been calculated in [44] when both the parameters of every crack are described by interval variables. Cracked structures with limited uncertain data have been investigated to estimate time-dependent reliability by modeling the fatigue crack propagation assuming the crack length as an interval variable and fixing the number of fatigue load cycles [45,46]. Recently the dynamic response of multi-cracked beams with cracks depth modelled as interval variables has been evaluated both in the framework of continuous beam theory [47] by proposing an explicit formulation and by performing a generalized modal analysis adopting a finite element model [48,49].

Within this context and building on the latter recent work [49], the present paper deals with the response of linear elastic truss-like and frame-like structures with damaged members where crack depths are modeled as uncertain variables. Crack is modelled by introducing a local compliance that produces a discontinuity of displacements in correspondence of the cracked section. The compliance of the cracked member is obtained by adding the compliance of the intact element to the overall compliance due to the crack. Considering the lack of information about probability distribution of the crack severity, damage extent is modeled as an uncertain-but-bounded variable according to the interval analysis. Dynamic governing equations are solved considering the mass matrix as a deterministic quantity, while stiffness and damping matrices as uncertain matrices depending on the crack extension.

The time-varying bounds of the response of the damaged structures are therefore evaluated as the minimum and maximum, at each time instant, between the responses calculated by performing two parallel deterministic modal analyses associated to two combinations of the extreme values of interval uncertainties, generally the so-called trivial combinations (fixing all the parameters at their upper bounds and lower bounds, respectively) [49]. The two modal analyses require in turn the solution of two generalized eigenvalue problems and the step-by-step integration of two corresponding deterministic equations of motion in the modal sub-space. Moreover, taking full advantage of the pseudo-static sensitivity analysis recently introduced to treat structures with uncertain-but-bounded mechanical properties [50], a preliminary test is conducted to seek the two most common combinations of the endpoints of the interval parameters over the time interval of interest to be eventually used in the modal analysis instead of the trivial ones.

The proposed approach allows to provide the lower and upper bounds of the selected displacement component with a remarkable reduction of the computational cost considering only two deterministic analyses whatever the number of uncertain parameters involved.

Numerical tests on 2D and 3D truss and frame structures with multiple cracks with uncertain-but-bounded depths and subjected to

different excitations highlight the potentialities of the method, considering an increasing level of uncertainty.

Entering into the details of the exposition, the next section accounts for the governing equations of the problem, in particular the crack model description for truss and frame members is reported. The proposed method to handle the interval uncertainties in the cracks depths is outlined in Section 3 and in Section 4 the solution procedure is validated through several numerical tests. Conclusions are drawn in Section 5. Finally an Appendix is included.

2. Formulation of the problem

2.1. Crack model description: truss member

Consider a linear elastic truss structure subjected to a dynamic load. The displacement vector for the generically oriented i-th bar element of length L_i, mass density ρ, elastic modulus E, rectangular cross-section $B_i \times H_i$, cross-sectional area A_i, which connects node 1 to node 2 is given in the global coordinate systems by

$$\mathbf{u}_i(t) = [\, u_1(t) \quad v_1(t) \quad u_2(t) \quad v_2(t) \,]^{\mathrm{T}} \tag{1}$$

where the symbol T denotes transpose vector/matrix and u and v represent the displacements in the x and z directions, respectively (see Fig. 1).

The axial compliance of the i-th bar is indicated with c_i. Consider that the i-th element of the truss structure is damaged with a crack of depth a_i (see Fig. 1). In presence of damage in the i-th truss member, an additional axial compliance, named c_i^{crack}, is added to the intact axial one defined by c_i^{intact}. The c_i^{intact} expression for an intact, homogeneous bar with a constant cross-section is given by

$$c_i^{intact} = L_i / (EA_i) \tag{2}$$

The additional compliance $c_i^{crack}(a_i)$ can be expressed by the following expression:

$$c_i^{crack}(a_i) = \frac{2(1-\nu^2)}{E} \int_0^{A_{crack}} \left(\frac{K_{IN}(a_i)}{N} \right)^2 \mathrm{d}A_{crack} \tag{3}$$

where A_{crack} represents the cracked area, ν is the Poisson's ratio, N is the axial force while K_{IN} is the Mode I stress intensity factor [51] given by:

$$K_{IN}(a_i) = \frac{N}{B_i H_i} \sqrt{\pi a_i} F_N(\gamma_i) \tag{4}$$

with $\gamma_i = a_i / H_i$ the non dimensional crack depth.

The term $F_N(\gamma_i)$ in Eq. (4) is a correction function which takes the following expression (see [52]):

$$F_N(\gamma_i) = 1.12 - 0.23\gamma_i + 10.6(\gamma_i)^2 - 2.17(\gamma_i)^3 + 30.4(\gamma_i)^4 \tag{5}$$

Then the total axial compliance of the i-th cracked bar element takes the following form:

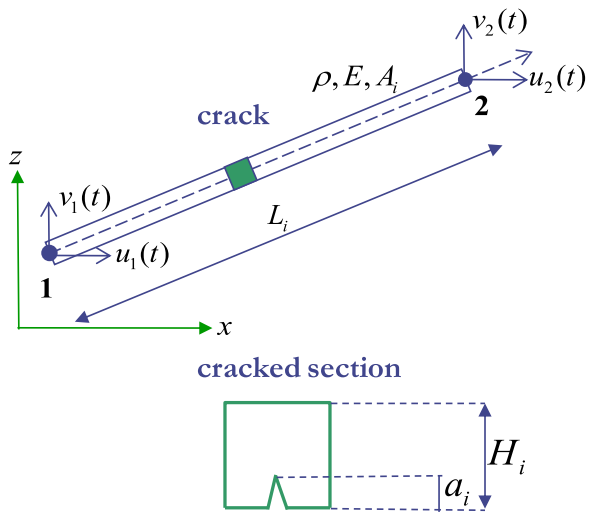

Fig. 1. Planar truss element with an open-edge crack.

$$c_i(a_i) = c_i^{intact} + c_i^{crack}(a_i) \tag{6}$$

and the stiffness matrix of the bar element with an open edge crack is given by:

$$\mathbf{K}_i(a_i) = \mathbf{G}_i^{\mathrm{T}} c_i(a_i)^{-1} \mathbf{G}_i \tag{7}$$

where $c_i(a_i)^{-1}$ is the inverse of the compliance $c_i(a_i)$ given in Eq. (6), while $\mathbf{G}_i$ is the element compatibility matrix expressed as:

$$\mathbf{G}_i = [\,1 \quad 0 \quad -1 \quad 0\,] \tag{8}$$

Using the rotation matrix $\mathbf{R}_i$, which takes into account the inclination of the generic bar, the matrices for the truss elements in the global coordinate system can be straightforwardly evaluated.

For three-dimensional truss structures, the displacement vector for the generically oriented i-th bar element (length L_i and rectangular cross-sectional area A_i) connecting node 1 to node 2 in the global coordinate systems takes the following form:

$$\mathbf{u}_i(t) = [\,u_1(t) \quad v_1(t) \quad w_1(t) \quad u_2(t) \quad v_2(t) \quad w_2(t)\,]^{\mathrm{T}} \tag{9}$$

where u, v and w are the three displacements in the x, z and y directions, respectively.

All of the previously reported steps for evaluating the stiffness matrix of the damaged member are confirmed. The only modification to be introduced for the spatial case consists in the passage from the elementary stiffness matrix in local coordinates to the stiffness matrix in global coordinates by suitably defining the rotation matrix $\mathbf{R}_i$.

2.2. Crack model description: frame member

Consider a generically oriented i-th beam element of length L_i, mass density ρ, Young's modulus E and cross-sectional area A_i, which connects node 1 to node 2 (see Fig. 2). The vector of the nodal displacements for the beam element is:

$$\mathbf{u}_i(t) = [\,u_1(t) \quad v_1(t) \quad \psi_1(t) \quad u_2(t) \quad v_2(t) \quad \psi_2(t)\,]^{\mathrm{T}} \tag{10}$$

where at a local node the displacement has two translational components u and v in the x and z directions and a rotational component ψ.

The beam presents a crack of depth a_i at distance $\xi_i L_i$ from node 1 (see Fig. 2). The flexibility matrix $\mathbf{C}_i(a_i)$ of the damaged beam element is given by the sum of the flexibility matrix of the intact element $\mathbf{C}_i^{int}$ and an additional flexibility matrix $\mathbf{C}_i^{crack}(a_i)$ given by the presence of the crack:

$$\mathbf{C}_i(a_i) = \mathbf{C}_i^{int} + \mathbf{C}_i^{crack}(a_i) \tag{11}$$

In particular, the matrix $\mathbf{C}_i^{int}$ has the following form:

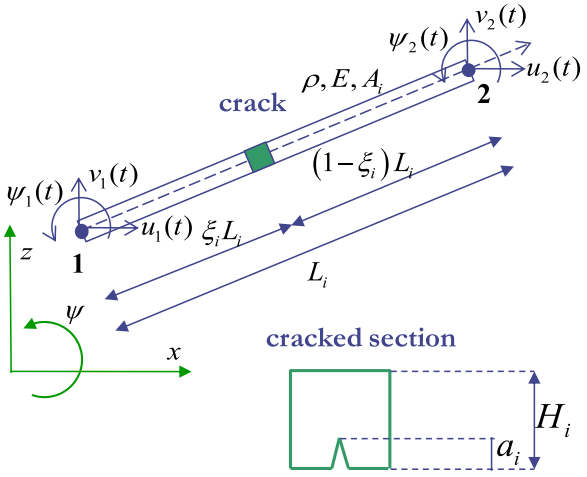

Fig. 2. Planar frame element with an open-edge crack.

$$\mathbf{C}_i^{intact} = \begin{bmatrix} \frac{L_i}{EA_i} & 0 & 0 \\ 0 & \frac{L_i}{EI_i} & 0 \\ 0 & 0 & \frac{L_i}{3EI_i} \end{bmatrix} \tag{12}$$

where I_i is the moment of inertia. The matrix $\mathbf{C}_i^{crack}(a_i)$ is given by:

$$\mathbf{C}_i^{crack}(a_i, \xi_i) = \begin{bmatrix} \lambda_N & \lambda_{NM} & (1-2\xi_i)\lambda_{NM} \\ \lambda_{NM} & \lambda_M & (1-2\xi_i)\lambda_M \\ (1-2\xi_i)\lambda_{NM} & (1-2\xi_i)\lambda_M & (1-2\xi_i)^2\lambda_M + (2/L_i)^2\lambda_S \end{bmatrix} \tag{13}$$

For the evaluation of the compliance coefficients $\lambda_N, \lambda_M, \lambda_{NM}$ and λ_S see details in Appendix.

The element stiffness matrix for the damaged beam is therefore given by

$$\mathbf{K}_i(a_i) = \mathbf{G}_i^{\mathrm{T}} \mathbf{C}_i(a_i)^{-1} \mathbf{G}_i \tag{14}$$

where $\mathbf{C}_i(a_i)$ is the matrix given in Eq. (11), while $\mathbf{G}_i$ is the element compatibility matrix, which for the case under exam takes the following form:

$$\mathbf{G}_i = \begin{bmatrix} -1 & 0 & 0 & 1 & 0 & 0 \\ 0 & 0 & -1 & 0 & 0 & 1 \\ 0 & -2/L_i & -1 & 0 & 2/L_i & -1 \end{bmatrix} \tag{15}$$

Then the rotation matrix $\mathbf{R}_i$ for a frame element transforms the 6×6 matrix $\mathbf{K}_i(a_i)$ into another 6×6 stiffness matrix of the damaged beam defined in the global coordinate system.

In the three-dimensional setting, the vector of the nodal displacement reads

$$\mathbf{u}_i(t) = [\, u_1 \quad v_1 \quad w_1 \quad \psi_{x1} \quad \psi_{z1} \quad \psi_{y1} \quad u_2 \quad v_2 \quad w_2 \quad \psi_{x2} \quad \psi_{z2} \quad \psi_{y2} \,]^{\mathrm{T}} \tag{16}$$

where the dependence of the all displacement components by the time t is omitted.

The only difference between a 2D frame element and a 3D frame element consists in the number of DOFs at each node that is six at each node, specifically three translational displacements in the x, z and y directions, and three rotations with respect to the x, z and y axes. In the local coordinate system the x-axis coincides with the geometrical axis and the z- and y- axes are the principal axes of the cross-section.

In presence of a beam element with an edge crack of depth a_i located at a distance $\xi_i L_i$ from the node 1 the flexibility matrix is given again by the sum of the two contributions, namely the matrix $\mathbf{C}_i^{int}$ related to the intact beam and the matrix $\mathbf{C}_i^{crack}(a_i)$ accounting for the damage (see Eq. (11)).

For the three-dimensional case, the compatibility matrix $\mathbf{C}_i^{int}$ takes the following form:

$$\mathbf{C}_i^{intact} = \begin{bmatrix} \frac{L_i}{GJ_{t_i}} & 0 & 0 & 0 & 0 & 0 \\ 0 & \frac{L_i}{3EI_{z_i}} & -\frac{L_i}{6EI_{z_i}} & 0 & 0 & 0 \\ 0 & -\frac{L_i}{6EI_{z_i}} & \frac{L_i}{3EI_{z_i}} & 0 & 0 & 0 \\ 0 & 0 & 0 & \frac{L_i}{3EI_{y_i}} & -\frac{L_i}{6EI_{y_i}} & 0 \\ 0 & 0 & 0 & -\frac{L_i}{6EI_{y_i}} & \frac{L_i}{3EI_{y_i}} & 0 \\ 0 & 0 & 0 & 0 & 0 & \frac{L_i}{EA_i} \end{bmatrix} \tag{17}$$

where GJ_{t_i}/L_i is the torsional stiffness of the i-th beam with G shear modulus, EA_i/L_i is the axial stiffness with E Young modulus, I_{z_i} and I_{y_i} are the moments of inertia with respect the axes z and y.

The additional compliance matrix $\mathbf{C}_i^{crack}(a_i)$ is evaluated as:

$$\mathbf{C}_i^{crack}(a_i) = \mathbf{T}_i^{\mathrm{T}}(\xi_i) \widehat{\mathbf{C}}_i^{crack}(a_i) \mathbf{T}_i(\xi_i) \tag{18}$$

In Eq. (18) $\mathbf{T}_i$ represents the transformation matrix for the generic i-th frame element depending by the non dimensional crack location ξ_i and has the following expression:

$$\mathbf{T}_i = \begin{bmatrix} 0 & 0 & 0 & 0 & 0 & 1 \\ 0 & 0 & 0 & 1/L_i & 1/L_i & 0 \\ 0 & -1/L_i & -1/L_i & 0 & 0 & 0 \\ 1 & 0 & 0 & 0 & 0 & 0 \\ 0 & 1-\xi_i & -\xi_i & 0 & 0 & 0 \\ 0 & 0 & 0 & \xi_i - 1 & \xi_i & 0 \end{bmatrix} \tag{19}$$

while the local compliance matrix $\widehat{\mathbf{C}}_i^{crack}(a_i)$ reads:

$$\widehat{\mathbf{C}}_i^{crack}(a_i) = \begin{bmatrix} \lambda_N & 0 & 0 & 0 & 0 & \lambda_{NM_y} \\ 0 & \lambda_{S_z} & 0 & 0 & 0 & 0 \\ 0 & 0 & \lambda_{S_y} & \lambda_{S_yT_x} & 0 & 0 \\ 0 & 0 & \lambda_{S_yT_x} & \lambda_{T_x} & 0 & 0 \\ 0 & 0 & 0 & 0 & \lambda_{M_z} & 0 \\ \lambda_{NM_y} & 0 & 0 & 0 & 0 & \lambda_{M_y} \end{bmatrix} \tag{20}$$

where $\lambda_N, \lambda_{S_z}, \lambda_{S_y}, \lambda_{M_z}, \lambda_{M_y}$ and λ_{T_x} are the axial compliance related to the axial force N, the shear compliances related to the shear forces S_z and S_y, respectively; the bending compliances related to the bending moments M_z and M_y, respectively; and the torsional compliance related to the torque T_x. Moreover in Eq. (20) the coupled compliances $\lambda_{S_yT_x}$ and λ_{NM_y} take into account the coupling between the shear force S_y and the torque T_x and between the axial force N and the bending moment M_y. Details on the evaluation of the local compliances appearing in Eq. (20) are reported in Appendix.

Therefore the local stiffness matrix for the 3D frame element can be still calculated by Eq. (14) where $\mathbf{C}_i(a_i)$ is the matrix given in Eq. (11) whose final form is updated in terms of the two matrices $\mathbf{C}_i^{int}$ as $\mathbf{C}_i^{crack}(a_i)$ as reported in Eqs. (17) and (18) while $\mathbf{G}_i$ is the 3D frame element compatibility matrix taking the following form:

$$\mathbf{G}_i = \begin{bmatrix} 0 & 0 & 0 & -1 & 0 & 0 & 0 & 0 & 0 & 1 & 0 & 0 \\ 0 & 0 & -1/L_i & 0 & 1 & 0 & 0 & 0 & 1/L_i & 0 & 0 & 0 \\ 0 & 0 & -1/L_i & 0 & 0 & 0 & 0 & 0 & 1/L_i & 0 & 1 & 0 \\ 0 & 1/L_i & 0 & 0 & 0 & 1 & 0 & -1/L_i & 0 & 0 & 0 & 0 \\ 0 & 1/L_i & 0 & 0 & 0 & 0 & 0 & -1/L_i & 0 & 0 & 0 & 1 \\ -1 & 0 & 0 & 0 & 0 & 0 & 1 & 0 & 0 & 0 & 0 & 0 \end{bmatrix} \tag{21}$$

Then the generic stiffness matrix for the i-th frame element needs to be transformed into the global coordinate system to account for the differences in orientation of all the frame members referred to the local coordinate systems.

2.3. Interval stiffness matrix for the damaged structure

Following a standard assembling procedure for both the truss-like and frame-like structures, the stiffness matrix $\mathbf{K}(\mathbf{a})$ of the whole structure with r damaged members depends on the vector $\mathbf{a} = [a_1 \quad a_2 \quad \cdots \quad a_r]^T$ collecting the r crack depths a_i ($i = 1,2,\ldots,r$).

Let us now to investigate the case in which the generic i-th crack a_i has an uncertain depth modeled as an uncertain-but-bounded variable.

Generally, following the interval symbolism of the classical interval analysis [26], an interval number α^I is represented by:

$$\alpha^I \in [\underline{\alpha}, \bar{\alpha}] = \{\alpha | \underline{\alpha} \le \alpha \le \bar{\alpha}, \alpha_i \in \mathbb{R}\} \tag{22}$$

where the apex I denotes the interval or uncertain-but-bounded number and $\underline{\alpha}$ and $\bar{\alpha}$ its lower and upper bounds, respectively. Similarly the interval number α^I can be expressed as

$$\alpha^I = \alpha_0 + \Delta\alpha e^I \tag{23}$$

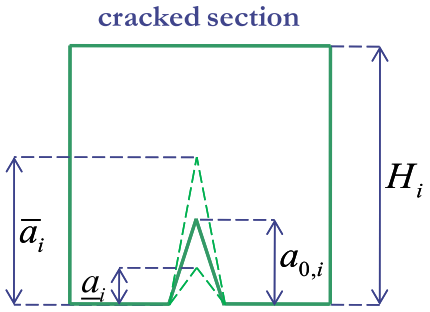

Fig. 3. Cracked section with depth of the crack modeled as uncertain-but-bonded variable.

in terms of midpoint α_0, deviation $\Delta\alpha$ and unitary interval e^I defined, respectively as

$$\alpha_0 = mid(\alpha) = \frac{\underline{\alpha} + \bar{\alpha}}{2};\ \Delta\alpha = \frac{\bar{\alpha} - \underline{\alpha}}{2};\ e^I = [-1, 1] \tag{24a,b,c}$$

By adopting the interval model, the generic crack depth $a_i^I = [\underline{a}_i, \bar{a}_i]$ can be expressed in the so-called affine form as

$$a_i^I = a_{0,i}\left(1 + \alpha_i^I\right) = a_{0,i}\left(1 + \Delta\alpha_i \widehat{e}_i^I\right) \tag{25}$$

with the assumption of symmetric fluctuations that implicates $\underline{\alpha}_i = -\bar{\alpha}_i$ and consequently $\alpha_{0,i} = 0$ (see Eqs. (23) and (24)). Therefore in Eq. (25) $a_{0,i}$ represents the deterministic nominal value of the crack depth for the i-th crack, $\Delta\alpha_i$ is the symmetric dimensionless fluctuation of the crack depth around its nominal value and $\widehat{e}_i^I = [-1, 1]$ represents the so-called extra unitary interval introduced in the improved interval analysis by Muscolino and Sofi [53] in order to treat variables with multiple occurrence of the same type as dependent ones and reduce the dependency phenomenon. Substituting $\widehat{\underline{e}}_i = -1$ in Eq. (25), the lower bound $\underline{a}_i$ of the crack depth is obtained, while substituting $\widehat{\bar{e}}_i = 1$ in Eq. (25), the upper bound depth $\bar{a}_i$ is derived (see Fig. 3). In presence of r cracked members, the vector $\mathbf{a}_0 = [\,a_{0,1} \quad a_{0,2} \quad \cdots \quad a_{0,r}\,]^{\mathrm{T}}$ of order $r \times 1$ collects the nominal values $a_{0,i}$, while the vector $\boldsymbol{\alpha} \in \boldsymbol{\alpha}^I = [\underline{\alpha}, \bar{\alpha}]$ with $\boldsymbol{\alpha}^I = \left[\,\alpha_1^I \quad \alpha_2^I \quad \cdots \quad \alpha_r^I\,\right]^{\mathrm{T}}$ collects the fluctuations $\alpha_i^I = \Delta\alpha_i \widehat{e}_i^I$ of the uncertain crack depths around their mean values.

Thus, in turn the global stiffness matrix $\mathbf{K}(\mathbf{a})$ becomes an interval matrix depending on the nominal values vector $\mathbf{a}_0$ and the fluctuations vector $\boldsymbol{\alpha}^I$ as:

$$\mathbf{K}\left(\mathbf{a}^I\right) = \mathbf{K}\left(\mathbf{a}_0, \boldsymbol{\alpha}^I\right) \tag{26}$$

2.4. Governing equation for structures with cracked members

The dynamics of a quiescent cracked structure with r damaged members modeled as interval variables under an external excitation $\mathbf{f}(t)$ is ruled by the following governing equation of motion:

$$\mathbf{M}\,\ddot{\mathbf{u}}\left(\mathbf{a}_0, \boldsymbol{\alpha}^I, t\right) + \mathbf{D}\left(\mathbf{a}_0, \boldsymbol{\alpha}^I\right)\dot{\mathbf{u}}\left(\mathbf{a}_0, \boldsymbol{\alpha}^I, t\right) + \mathbf{K}\left(\mathbf{a}_0, \boldsymbol{\alpha}^I\right)\mathbf{u}\left(\mathbf{a}_0, \boldsymbol{\alpha}^I, t\right) = \mathbf{f}(t) \tag{27}$$

In Eq. (27) $\mathbf{M}$ is the deterministic mass matrix of the structure which is not affected by the presence of the cracks and in turn by the uncertainty in the cracks depths; based on the previous considerations $\mathbf{K}(\mathbf{a}_0, \boldsymbol{\alpha}^I)$ is the stiffness matrix (see Eq. (27)) of the structure, depending on the uncertain cracks depths parameters.

In this paper, a proportional damping matrix (Rayleigh model) is considered so that the matrix $\mathbf{D}(\mathbf{a}_0, \boldsymbol{\alpha}^I)$ in Eq. (27) is expressed as a linear combination of the mass and stiffness matrices as:

$$\mathbf{D}\left(\mathbf{a}_0, \boldsymbol{\alpha}^I\right) = d_0\,\mathbf{M} + d_1\mathbf{K}\left(\mathbf{a}_0, \boldsymbol{\alpha}^I\right) \tag{28}$$

where d_0 and d_1 are the Rayleigh damping constants to be evaluated. This assumption accounts for the dependence of the damping matrix by the uncertainties collected in the vector $\boldsymbol{\alpha}^I$.

The interval vector $\mathbf{u}(\mathbf{a}_0, \boldsymbol{\alpha}^I, t)$ collects the $n \times 1$ nodal displacements, while symbol dot over a variable denotes differentiation with respect to time t.

3. Bounds of the cracked structure response

Objective of the interval analysis applied to the dynamic problem as expressed in Eq. (27) is the evaluation of the structural response in terms of bounds of the interval displacement vector collecting the dynamical response set at each instant, i.e.

$$\mathbf{u}\left(\mathbf{a}_0, \boldsymbol{\alpha}^I, t\right) = \left[\underline{\mathbf{u}}(\mathbf{a}_0, t),\ \bar{\mathbf{u}}(\mathbf{a}_0, t)\right] \tag{29}$$

being $\underline{\mathbf{u}}(\mathbf{a}_0, t)$ and $\bar{\mathbf{u}}(\mathbf{a}_0, t)$ the displacement lower and upper bound, respectively.

In the following the main steps of the procedure adopted to provide the bounds reported in Eq. (29) are summarized.

The presence of uncertain-but-bounded parameters affecting the stiffness matrix $\mathbf{K}(\mathbf{a}_0, \boldsymbol{\alpha}^I)$ requires in turn the solution of an interval eigenvalue problem expressed by:

$$\mathbf{K}\left(\mathbf{a}_0, \boldsymbol{\alpha}^I\right)\boldsymbol{\phi}_j\left(\mathbf{a}_0, \boldsymbol{\alpha}^I\right) = \lambda_j\left(\mathbf{a}_0, \boldsymbol{\alpha}^I\right)\mathbf{M}\,\boldsymbol{\phi}_j\left(\mathbf{a}_0, \boldsymbol{\alpha}^I\right);\quad (j = 1, 2, \cdots, m) \tag{30}$$

where $\lambda_j(\mathbf{a}_0, \boldsymbol{\alpha}^I) = \omega_j^2(\mathbf{a}_0, \boldsymbol{\alpha}^I)$ represents the j-th interval eigenvalue equivalent to the squared interval natural frequency and $\boldsymbol{\phi}_j(\mathbf{a}_0, \boldsymbol{\alpha}^I)$ is the associated interval eigenvector.

Among all possible eigenvalues satisfying Eq. (30) while the matrix $\mathbf{K}(\mathbf{a}_0, \boldsymbol{\alpha}^I)$ assumes all possible values within the interval defined by

$$\mathbf{K}\left(\mathbf{a}_0, \boldsymbol{\alpha}^I\right) = \left[\underline{\mathbf{K}}(\mathbf{a}_0), \bar{\mathbf{K}}(\mathbf{a}_0)\right] = \left\{\mathbf{K}(\mathbf{a}_0, \boldsymbol{\alpha}) \middle| \underline{k}_{ij}(\mathbf{a}_0) \le k_{ij}(\mathbf{a}_0) \le \bar{k}_{ij}(\mathbf{a}_0)\right\} \tag{31}$$

the first aim is to provide the narrowest eigenvalue interval i.e. [54–56,48,49]:

$$\lambda_j(\mathbf{a}_0, \boldsymbol{\alpha}) = \left[\underline{\lambda}_j(\mathbf{a}_0),\ \bar{\lambda}_j(\mathbf{a}_0)\right] \tag{32}$$

where $\underline{\lambda}_j(\mathbf{a}_0)$ and $\bar{\lambda}_j(\mathbf{a}_0)$ with $(j = 1, 2, \ldots, m)$, represent the LB and UB of the j-th interval eigenvalue.

The adopted method requires to solve the following two deterministic eigenvalue problems [56,49] defined by:

$$\begin{aligned} &\mathbf{K}(\mathbf{a}_0, \underline{\boldsymbol{\alpha}})\boldsymbol{\phi}_j^{(\mathrm{LB})}(\mathbf{a}_0) = \underline{\lambda}_j(\mathbf{a}_0)\,\mathbf{M}\,\boldsymbol{\phi}_j^{(\mathrm{LB})}(\mathbf{a}_0); \quad \boldsymbol{\phi}_j^{(\mathrm{LB})}(\mathbf{a}_0)^{\mathrm{T}}\,\mathbf{M}\,\boldsymbol{\phi}_k^{(\mathrm{LB})}(\mathbf{a}_0) = \Delta_{jk} \\ &\mathbf{K}(\mathbf{a}_0, \bar{\boldsymbol{\alpha}})\,\boldsymbol{\phi}_j^{(\mathrm{UB})}(\mathbf{a}_0) = \bar{\lambda}_j(\mathbf{a}_0)\mathbf{M}\,\boldsymbol{\phi}_j^{(\mathrm{UB})}(\mathbf{a}_0); \quad \boldsymbol{\phi}_j^{(\mathrm{UB})}(\mathbf{a}_0)^{\mathrm{T}}\,\mathbf{M}\,\boldsymbol{\phi}_k^{(\mathrm{UB})}(\mathbf{a}_0) = \Delta_{jk}, (j = 1, 2, \cdots m). \end{aligned} \tag{33a,b}$$

where Δ_{jk} is the Kronecker delta, $\boldsymbol{\phi}_j^{(\mathrm{LB})}(\mathbf{a}_0)$ and $\boldsymbol{\phi}_j^{(\mathrm{UB})}(\mathbf{a}_0)$ are the eigenvectors associated to the eigenproblem in which the two positions $\boldsymbol{\alpha} = \underline{\boldsymbol{\alpha}}$ (LB) and $\boldsymbol{\alpha} = \bar{\boldsymbol{\alpha}}$ (UB), are made respectively. The eigenvectors of both eigenproblems are real vectors, while the eigenvalues are real and positive quantities due to the circumstance that both the two stiffness matrices $\mathbf{K}(\mathbf{a}_0, \underline{\boldsymbol{\alpha}})$ and $\mathbf{K}(\mathbf{a}_0, \bar{\boldsymbol{\alpha}})$ as well as the mass matrix $\mathbf{M}$ are real, symmetric and positive definite matrices.

The solution of the double equation of motion provided by splitting Eq. (27) in terms of the combinations $\boldsymbol{\alpha} = \underline{\boldsymbol{\alpha}}$ and $\boldsymbol{\alpha} = \bar{\boldsymbol{\alpha}}$ of the uncertain parameters is performed by first introducing the two coordinate transformations in terms of the interval vector of modal displacement $\mathbf{q}(\boldsymbol{\alpha}^I, t)$ as follows:

$$\begin{aligned} &\mathbf{u}(\underline{\boldsymbol{\alpha}}, t) = \boldsymbol{\Phi}^{(\mathrm{LB})}(\mathbf{a}_0)\,\mathbf{q}(\underline{\boldsymbol{\alpha}}, t) \\ &\mathbf{u}(\bar{\boldsymbol{\alpha}}, t) = \boldsymbol{\Phi}^{(UB)}(\mathbf{a}_0)\,\mathbf{q}(\bar{\boldsymbol{\alpha}}, t) \end{aligned} \tag{34a,b}$$

where the matrices $\boldsymbol{\Phi}^{(\mathrm{LB})}(\mathbf{a}_0)$ and $\boldsymbol{\Phi}^{(\mathrm{UB})}(\mathbf{a}_0)$ collect in columns the eigenvectors $\boldsymbol{\phi}_j^{(\mathrm{LB})}(\mathbf{a}_0)$ and $\boldsymbol{\phi}_j^{(\mathrm{UB})}(\mathbf{a}_0)$, respectively.

The application of these coordinate transformations allows to project the equations of motion in the modal space as:

$$\begin{aligned} &\ddot{\mathbf{q}}(\underline{\boldsymbol{\alpha}}, t) + \underline{\boldsymbol{\Xi}}(\mathbf{a}_0)\,\dot{\mathbf{q}}(\underline{\boldsymbol{\alpha}}, t) + \underline{\boldsymbol{\Omega}}^2(\mathbf{a}_0)\,\mathbf{q}(\underline{\boldsymbol{\alpha}}, t) = \boldsymbol{\Phi}^{(\mathrm{LB})}(\mathbf{a}_0)^{\mathrm{T}}\,\mathbf{f}(t) \\ &\ddot{\mathbf{q}}(\bar{\boldsymbol{\alpha}}, t) + \bar{\boldsymbol{\Xi}}(\mathbf{a}_0)\,\dot{\mathbf{q}}(\bar{\boldsymbol{\alpha}}, t) + \bar{\boldsymbol{\Omega}}^2(\mathbf{a}_0)\,\mathbf{q}(\bar{\boldsymbol{\alpha}}, t) = \boldsymbol{\Phi}^{(UB)}(\mathbf{a}_0)^{\mathrm{T}}\,\mathbf{f}(t) \end{aligned} \tag{35a,b}$$

where $\underline{\boldsymbol{\Xi}}(\mathbf{a}_0)$ and $\bar{\boldsymbol{\Xi}}(\mathbf{a}_0)$ are the generalized diagonal damping matrices, which according to the Rayleigh model, can be written as:

$$\begin{aligned} &\underline{\boldsymbol{\Xi}}(\mathbf{a}_0) = d_0\,\mathbf{I}_m + d_1\,\underline{\boldsymbol{\Omega}}^2(\mathbf{a}_0) \\ &\bar{\boldsymbol{\Xi}}(\mathbf{a}_0) = d_0\,\mathbf{I}_m + d_1\,\bar{\Omega}^2(\mathbf{a}_0) \end{aligned} \tag{36a,b}$$

obtaining a set of decoupled differential equations; $\underline{\Omega}^2(\mathbf{a}_0)$ and $\bar{\Omega}^2(\mathbf{a}_0)$ are diagonal matrices whose $j-$ th element is $\underline{\lambda}_j(\mathbf{a}_0)$ and $\bar{\lambda}_j(\mathbf{a}_0)$, respectively.

By solving Eqs. (35a,b) in terms of vectors $\mathbf{q}(\underline{\boldsymbol{\alpha}}, t)$ and $\mathbf{q}(\bar{\boldsymbol{\alpha}}, t)$, the corresponding nodal responses can be calculated via the coordinate transformation previously introduced (Eqs. (34a,b)).

Lower and upper bounds of the k-th component of the interval dynamic response $\mathbf{u}(\mathbf{a}_0, \boldsymbol{\alpha}^I, t)$ can be evaluated by the following relationships:

$$\begin{aligned} &\underline{u}_k(\mathbf{a}_0, t) = \min\{\, u_k(\mathbf{a}_0, \underline{\boldsymbol{\alpha}}, t),\ \ u_k(\mathbf{a}_0, \underline{\boldsymbol{\alpha}}, t)\}; \\ &\bar{u}_k(\mathbf{a}_0, t) = \max\{\, u_k(\mathbf{a}_0, \underline{\boldsymbol{\alpha}}, t),\ \ u_k(\mathbf{a}_0, \bar{\boldsymbol{\alpha}}, t)\} \end{aligned} \tag{37a,b}$$

where the symbols $\min\{\cdot\}$ and $\max\{\cdot\}$ denote minimum (inferior) and maximum (superior) values, respectively.

It is worth to note that the two deterministic eigenvalue problems (see Eq. (33a,b)) are solved by selecting simultaneously all the uncertain-but-bounded parameters α_i^I for $i = 1,\ldots,r$ at their lower bounds $\underline{\alpha}_i$ collected in the vector $\boldsymbol{\alpha} = \underline{\boldsymbol{\alpha}}$ (see Eq. (33a)) and at their upper bounds $\bar{\alpha}_i$ collected in the vector $\boldsymbol{\alpha} = \bar{\boldsymbol{\alpha}}$ (see Eq. (33b)), namely the so-called "trivial combinations".

An improvement on the accuracy in the solution of the eigenvalues problems in Eqs. (33) could be achieved by resorting to an alternative method recently proposed by Muscolino et al. [50]. Specifically in Ref. [50] it is presented a procedure based on a preliminary pseudo-static sensitivity analysis allowing to identify suitable combinations of the endpoints of the uncertain parameters, called "most common combinations", which can be potentially employ to define the vectors $\boldsymbol{\alpha} = \underline{\boldsymbol{\alpha}}$ and $\boldsymbol{\alpha} = \bar{\boldsymbol{\alpha}}$ in replacement of the trivial ones.

The pseudo-static sensitivity functions of the time-varying displacement with respect to the i-th uncertain parameter are collected in the vector $\mathbf{s}_{u,i}(t)$ evaluated as follows:

$$\mathbf{s}_{u,i}(t) = \left.\frac{\partial \mathbf{u}(\mathbf{a}_0, t)}{\partial \alpha_i}\right|_{\boldsymbol{\alpha}=\mathbf{0}} = -\mathbf{K}(\mathbf{a}_0)\mathbf{K}_i\mathbf{u}(\mathbf{a}_0, \boldsymbol{\alpha}, t) \text{ with } i = 1, 2, \ldots, r \tag{38}$$

where

$$\mathbf{K}_i = \left.\frac{\partial \mathbf{K}(\mathbf{a}_0, \boldsymbol{\alpha}, t)}{\partial \alpha_i}\right|_{\boldsymbol{\alpha}=\mathbf{0}} \tag{39}$$

and $\mathbf{u}(\mathbf{a}_0, t)$ is the nominal displacement vector (i.e. $\boldsymbol{\alpha} = \mathbf{0}$) solution of the governing equation of motion (see Eq. (27)) where all the

matrices are set at their deterministic values, namely $\mathbf{D}(\mathbf{a}_0)$ and $\mathbf{K}(\mathbf{a}_0)$, and provided by performing the classical modal analysis.

The knowledge of the pseudo-static sensitivities $s_{u_{k,i}}(t)$ of the k-th displacement component $u_k(\mathbf{a}_0, \boldsymbol{\alpha}^I, t)$ with respect to the i-th uncertain parameter at each time instant t allows to estimate the combinations of the extreme values of the i-th uncertain parameter, namely $\alpha_{k,i}^{(\mathrm{LB})}(t)$ and $\alpha_{k,i}^{(\mathrm{UB})}(t)$ providing the LB and UB of the selected k-th displacement component.

By analysing the sign of $s_{u_{k,i}}(t)$, $\alpha_{k,i}^{(\mathrm{LB})}(t)$ and $\alpha_{k,i}^{(\mathrm{UB})}(t)$ can be evaluated as

$$\begin{aligned} &\text{if } s_{u_{k,i}}(t) > 0, \quad \text{then } \alpha_{k,i}^{(\mathrm{UB})}(t) = \bar{\alpha}_i(t), \quad \alpha_{k,i}^{(\mathrm{LB})}(t) = \underline{\alpha}_i(t); \\ &\text{if } s_{u_{k,i}}(t) < 0, \quad \text{then } \alpha_{k,i}^{(\mathrm{UB})}(t) = \underline{\alpha}_i(t), \quad \alpha_{k,i}^{(\mathrm{LB})}(t) = \bar{\alpha}_i(t), \quad (k = 1, \cdots, n; i = 1, \cdots, r). \end{aligned} \tag{40a,b}$$

Finally, for a fixed k-th displacement component the more effective time independent combinations are evaluated simply by using the Mathematica® [57] function "Commonest":

$$\begin{aligned} &\underset{\sim}{\boldsymbol{\alpha}} C, k = \underset{0 \le t \le t_F}{\mathrm{Commonest}}\left\{ \alpha_{k,1}^{(\mathrm{LB})}(t) \quad \alpha_{k,2}^{(\mathrm{LB})}(t) \quad \cdots \quad \alpha_{k,r}^{(\mathrm{LB})}(t) \right\}; \\ &\underset{\sim}{\tilde{\boldsymbol{\alpha}}}_{C,k} = \underset{0 \le t \le t_F}{\mathrm{Commonest}}\left\{ \alpha_{k,1}^{(\mathrm{UB})}(t) \quad \alpha_{k,2}^{(\mathrm{UB})}(t) \quad \cdots \quad \alpha_{k,r}^{(\mathrm{UB})}(t) \right\}, \quad (k = 1, 2, \cdots, n). \end{aligned} \tag{41a,b}$$

and then evaluate the eigenproperties and perform the two parallel generalized interval modal analyses (see Eqs. (33)-(35)) associated to the most common combinations of the bounds of the interval parameters conveniently updating the combinations $\boldsymbol{\alpha} = \underline{\boldsymbol{\alpha}}$ and $\boldsymbol{\alpha} = \bar{\boldsymbol{\alpha}}$ with $\boldsymbol{\alpha} = \underset{\sim}{\boldsymbol{\alpha}} C, k$ and $\boldsymbol{\alpha} = \underset{\sim}{\tilde{\boldsymbol{\alpha}}}_{C,k}$.

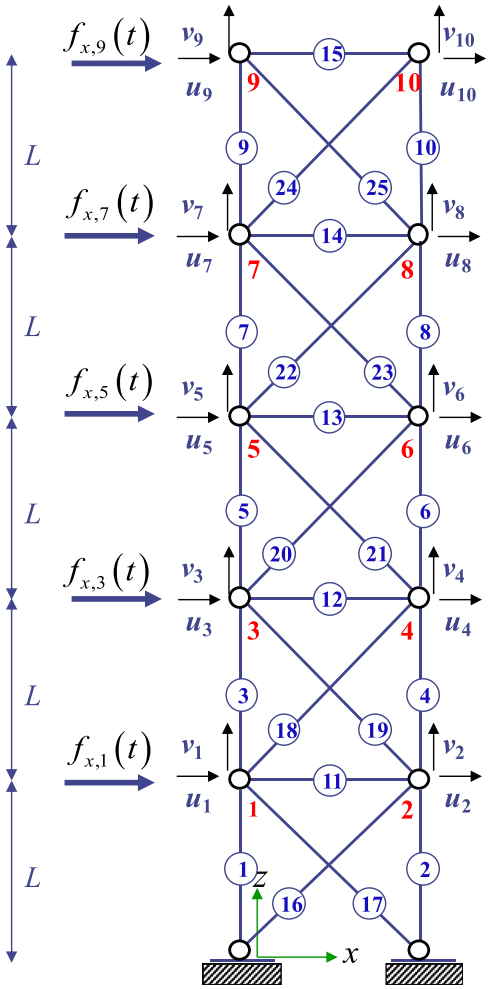

Fig. 4. 2D 25-bar truss structure: geometry and load condition.

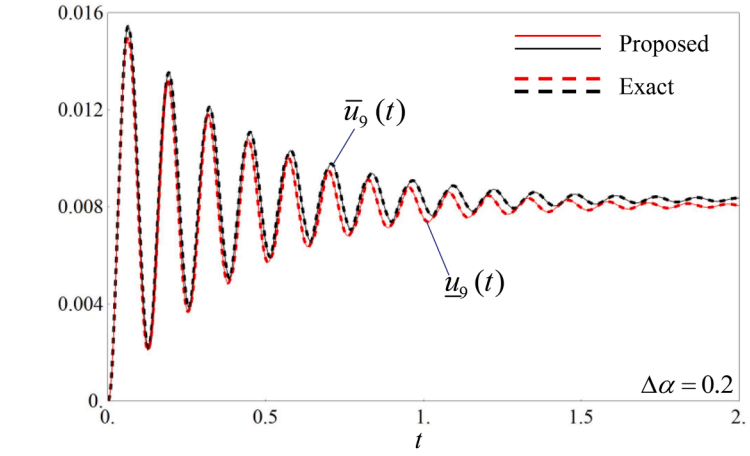

a)

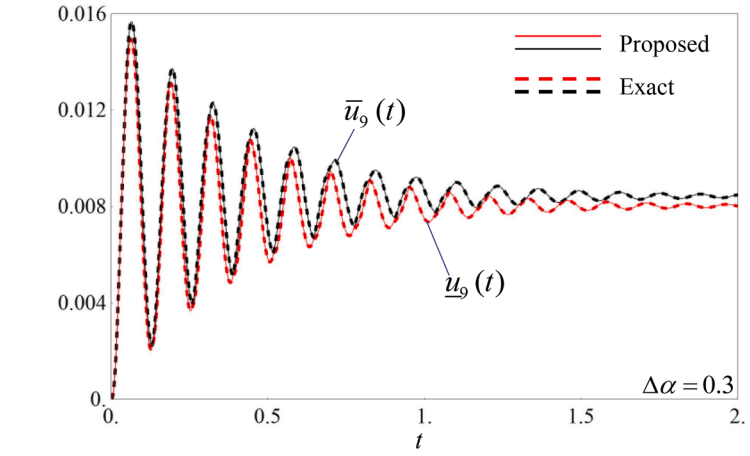

b)

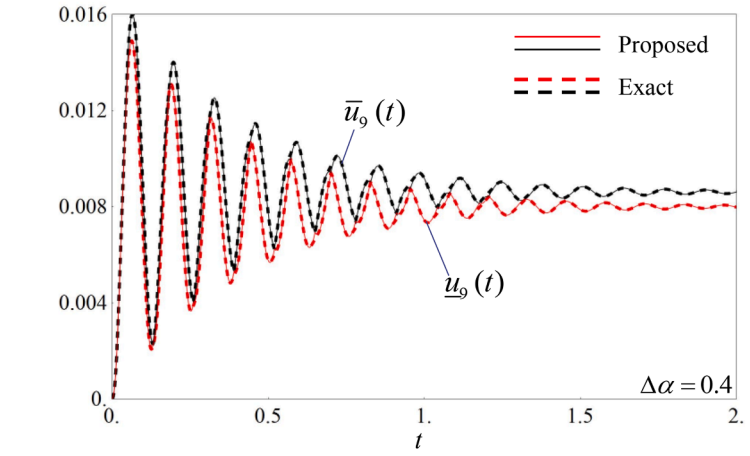

c)

Fig. 5. Time-varying lower and upper bounds of the 9-th node displacement in *x*-direction (in m) of the 2D multi-cracked truss structure ($i = 1,2,\ldots,10$) subjected to UnitStep functions: proposed method (continuous lines) and exact solution (dotted lines) for a) $\Delta\alpha = 0.2$, b) $\Delta\alpha = 0.3$ and c) $\Delta\alpha = 0.4$.

4. Numerical applications

In this section, the performance of the present procedure on uncertain cracked trusses and frames is illustrated through some numerical applications. For comparison, the results of a combinatorial procedure, known as vertex method [31,58,59] combined with those obtained by the Monte Carlo (MC) method [31,60] are also included.

The vertex method and the Monte Carlo method as developed in the interval framework are both the reference solutions for analysis with uncertainties under the assumption of monotonicity behavior and for the general case of non-monotonic dependence on the parameters.

Specifically, the mentioned vertex method consists in performing 2^r deterministic analyses, at each time instant, exploring all possible combinations of the extreme values of the r uncertain parameters in input. Despite its computational effort, this method represents the most robust procedure to handle problems with interval parameters when the response is a monotonic function of the interval uncertainties involved, returning exact bounds of the response function in correspondence to a proper combination (among the 2^r being r the number of interval parameters). Due to its philosophy, the vertex method does not guarantee accuracy if the behavior of the response function is not monotonic with respect to uncertain parameters. Alternatively the MC method considers the uncertain-but-bounded parameters as uniform distributed variables in their respective intervals. This representation allows to take into account also values falling within the range that defines the generic uncertain parameter.

Thus the combinatorial vertex-MC procedure, referred as the exact one, consists in the evaluation of the minimum and maximum at each time instant among the 2^r + MC samples combinations, allowing to catch also parameters values within the intervals and therefore to take into account the possible no-monotonic behavior with respect to the uncertain parameters of the structural response along the time window considered.

4.1. Truss-like structure with uncertain damage

The first analysis is conducted on a steel 25-bar truss structure (see Fig. 4) subjected to horizontal forces applied at the nodes 1,3,5,7 and 9 in the x-direction namely $f_{x,j}(t)$ with $j = 1,3,5,7,9$.

All the bars are assumed to have cross-sectional area $A_i = A = 0.01$ m^2 (prismatic section with B_i=H_i=0.1 m $\forall i$) with $i = 1, 2, \ldots, 25$ and lengths L_i deducible from Fig. 4 where $L = 5.1$ m. Young modulus and Poisson ratio are $E = 2.1 \times 10^8$ kN/m^2 and $\nu = 0.3$ respectively.

Furthermore, each node possesses a lumped mass $M = 500$ kg. All the vertical bars are supposed to be damaged ($r = 10$) with crack depths modeled as interval parameters $a_i^I = a_{0,i}(1 + \Delta\alpha_i e_i^I)(i = 1, 2, \ldots, 10)$ with nominal value $a_{0,i} = a_0 = 0.4H$ $\forall i$ and deviation amplitudes $\Delta\alpha_i = \Delta\alpha$. The effect of the uncertainty in the cracks depth is explored for increasing values of the deviation amplitude considering $\Delta\alpha_i = \Delta\alpha = 0.2, 0.3$ and 0.4.

Without loss of generality, the Rayleigh damping constants d_0 and d_1 were evaluated relating to the damaged mean configuration using as reference the mean stiffness matrix defined as $\mathbf{K}(\mathbf{a}_0)| = \mathbf{K}(\mathbf{a}_0, \boldsymbol{\alpha})|_{\boldsymbol{\alpha}=\mathbf{0}}$, see Eq. (26). As a consequence, in Eq. (28) the values $d_0 = 4.09071 s^{-1}$ and $d_1 = 0.000347 s$ are derived in such a way that the modal damping ratio for the first and second modes of the nominal structure is $\zeta_0 = 0.05$.

The first results concern the truss structure response subjected to UnitStep functions, namely $f_{x,j}(t) = F_0 U(t)$ ($j = 1,3,5,7,9$) with $F_0 = 15$ kN and $U(t) = 1$ for $t \geq 0$ by focusing the attention on the 9-th node displacement in x-direction, namely $u_9^I(t)$.

By applying the pseudo-static sensitivity analysis, the calculated commonest combinations in the considered time window for the 9-th node displacement in x-direction component coincide with the trivial combinations for all the uncertain parameters; that is the Eqs. (41a,b) in the case under exam take the following forms:

$$\underset{\sim}{\boldsymbol{\alpha}}\, C, u_9 = \left[\underline{\alpha}_{u_9,1} \quad \underline{\alpha}_{u_9,2} \quad \cdots \quad \underline{\alpha}_{u_9,10}\right]$$
$$\underset{\sim}{\tilde{\boldsymbol{\alpha}}}_{C,u_9} = \left[\bar{\alpha}_{u_9,1}\, \bar{\alpha}_{u_9,2} \cdots \bar{\alpha}_{u_9,10}\right] \tag{42a,b}$$

Figs. 5a, 5b and 5c show the time-varying bounds of the 9-th node displacement in x-direction, obtained by applying the procedure explained in Section 3.

The bounds provided by the proposed method (continuous lines in Fig. 5) are compared with the bounds of the reference solution (dotted lines in Fig. 5) evaluated by combining the results of the vertex method evaluated by the solving $2^{r=10} = 1024$ problems, with the results obtained by the MC (1000 samples). It is worth to note the excellent agreement between the bounds evaluated by the two procedures for all the levels of uncertainty.

Analogous results are provided considering the damaged truss structure subjected to impulsive load with $f_{x,j}(t) = F_0\delta(t)$ ($j = 1,3,5,7,9$) with $F_0 = 15$ kN and $\delta(t)$ the Dirac delta function.

The parameters combinations provided by applying the preliminary pseudo-sensitivity analysis for this second load scenario and the displacement component $u_9(t)$ are collected in the following vectors:

$$\underset{\sim}{\boldsymbol{\alpha}}\, C, u_9 = \left[\underline{\alpha}_{u_9,1} \quad \cdots \quad \bar{\alpha}_{u_9,7} \cdots \underline{\alpha}_{u_9,10}\right]$$
$$\underset{\sim}{\tilde{\boldsymbol{\alpha}}}_{C,u_9} = \left[\bar{\alpha}_{u_9,1} \cdots \underline{\alpha}_{u_9,7} \cdots \bar{\alpha}_{u_9,10}\right] \tag{43a,b}$$

It is worth to note that the commonest combinations of the uncertain parameters coincide with the trivial ones with the exception of

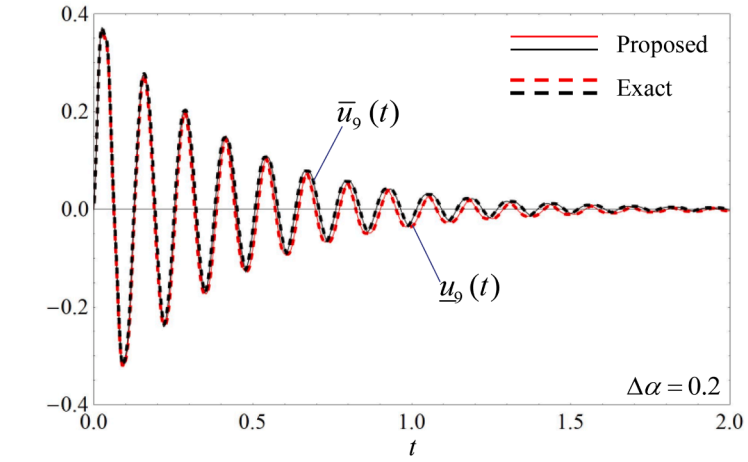

a)

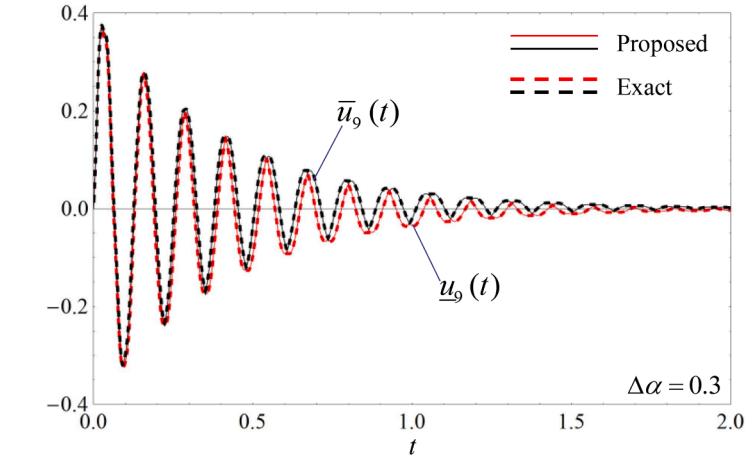

b)

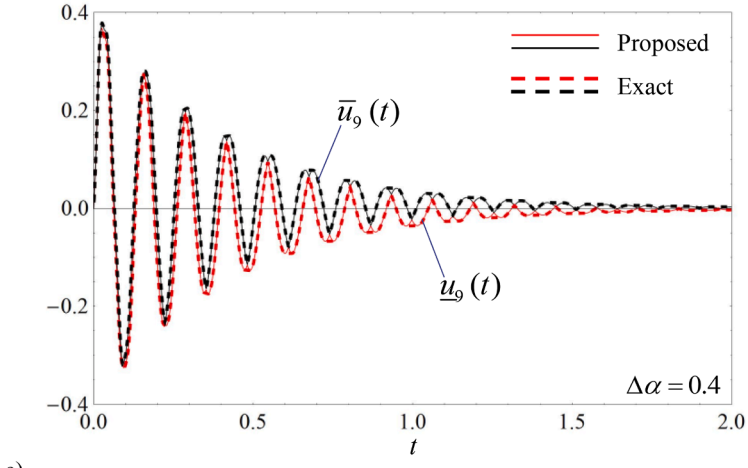

c)

Fig. 6. Time-varying lower and upper bounds of the 9-th node displacement in x-direction (in m) of the 2D multi-cracked truss structure ($i = 1,2,\ldots,10$) subjected to impulsive functions: proposed method (continuous lines) and exact solution (dotted lines) for a) $\Delta\alpha = 0.2$, b) $\Delta\alpha = 0.3$ and c) $\Delta\alpha = 0.4$.

the seventh uncertain parameter, namely the crack depth in the seventh vertical cracked member (see Fig. 4).

In Figs. 6a, 6b and 6c the time histories of the LB and UB of the interval nodal displacement $u_9^I(t)$ are reported for the three selected deviation amplitude values. Once more the bounds provided by applying the proposed procedure are compared with the ones calculated via the vertex method ($2^{r=10} = 1024$ deterministic dynamic analyses) combined with the MC (1000 samples). The graphs show the good accuracy of the proposed procedure also for high level of uncertainty.

A second application concerns a 3D 26-bar truss structure with 18 DOFs (see Fig. 7) constrained in the *x, y* and *z* directions at the bottom four corners (namely the nodes 1, 2, 3 and 4). All the truss members have the same rectangular cross-section with $B = H = 0.06$ m. Assume the truss structure is made of steel with mechanical properties $E = 2.1 \times 10^8$ kN/m^2 and $\nu = 0.3$, respectively. The geometry is defined by the $L = 6$ m dimension in plan and by the H_1=3 m and H_2=3.5 m dimensions in height as reported in Fig. 7.

The 3D truss is subjected to a horizontal force in *y*-direction (*yz* plane) applied at the node 9, namely $f_{y,9}(t)$. Furthermore, each node possesses a lumped mass $M = 500$ kg.

The analyzed damage scenario involves the first $r = 13$ bars as numbered in Fig. 7 with crack depth for the *i*-th member modeled as interval variable $a_i^I = a_{0,i}(1 + \Delta\alpha_i e_i^I)$ with nominal depth $a_{0,i} = a_0 = 0.4H$ and deviation amplitude $\Delta\alpha_i = \Delta\alpha \ \forall i$ ($i = 1, 2, \ldots, 13$). As in the previous case, the values of the Rayleigh damping constants $d_0 = 12.6971 s^{-1}$ and $d_1 = 0.000197 s$ are derived in such a way that the modal damping ratio for the first and second modes of the nominal damaged structure is $\zeta_0 = 0.05$.

First the truss structure response is evaluated considering a UnitStep function acting at node 9, that is $f_{y,9}(t) = F_0 U(t)$ with $F_0 = 150$ *k*N and $U(t) = 1$ for $t \geq 0$ and the interval displacement of node 10 in *z*-direction $v_{10}^I(t)$ is selected as quantity of interest.

The application of the pseudo-static sensitivity procedure returns for the displacement $v_{10}(t)$ the following commonest combinations:

$$\underset{\sim}{\boldsymbol{\alpha}}_{C,v_{10}} = \left[\underline{\alpha}_{v_{10},1} \quad \underline{\alpha}_{v_{10},2} \quad \bar{\alpha}_{v_{10},3} \quad \cdots \quad \bar{\alpha}_{v_{10},7}\, \bar{\alpha}_{v_{10},8} \cdots \underline{\alpha}_{v_{10},13}\right]$$
$$\tilde{\boldsymbol{\alpha}}_{C,v_{10}} = \left[\bar{\alpha}_{v_{10},1}\, \bar{\alpha}_{v_{10},2}\, \underline{\alpha}_{v_{10},3} \quad \cdots \quad \underline{\alpha}_{v_{10},7} \quad \underline{\alpha}_{v_{10},8} \cdots \bar{\alpha}_{v_{10},13}\right] \tag{44a,b}$$

which differ by the trivial ones for the third, seventh and eighth parameters that are the uncertain crack depths in the damaged members 3, 7 and 8, respectively (see Fig. 7).

LB and UB of $v_{10}(t)$ evaluated as proposed in Section 3 are reported in Figs. 8a, 8b and 8c for increasing values of the deviation amplitude ($\Delta\alpha_i = \Delta\alpha = 0.2, 0.3$ and 0.4). For comparison purpose LB and UB of $v_{10}(t)$ are also calculated via the reference procedure which requires the solution of $2^{r=13} = 8192$ problems to combine with the results obtained by the MC (1000 samples). From the

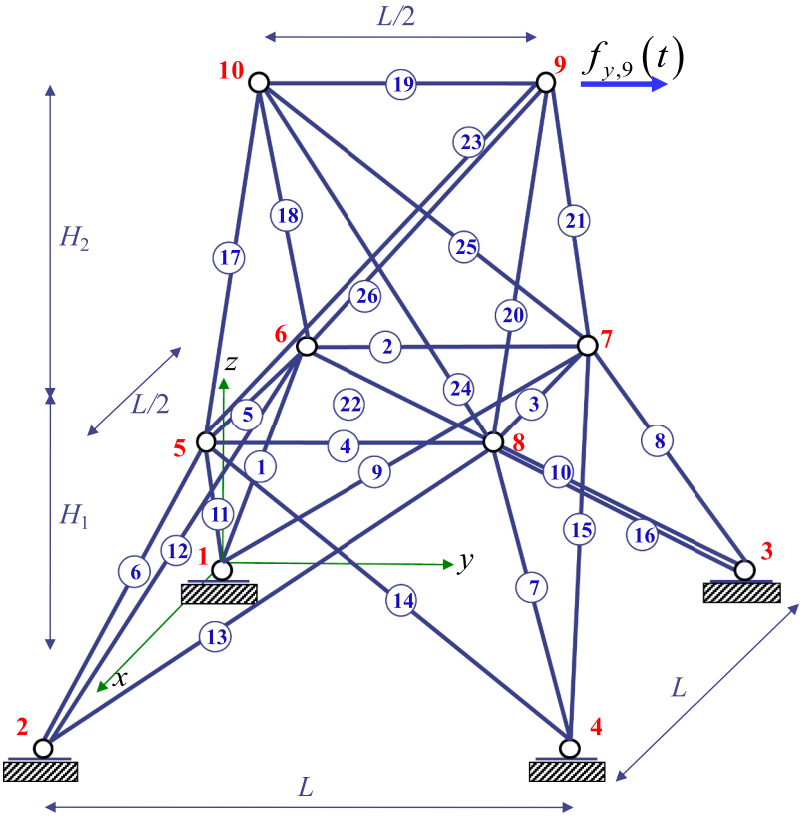

Fig. 7. 3D 26-bar truss structure: geometry and load condition.

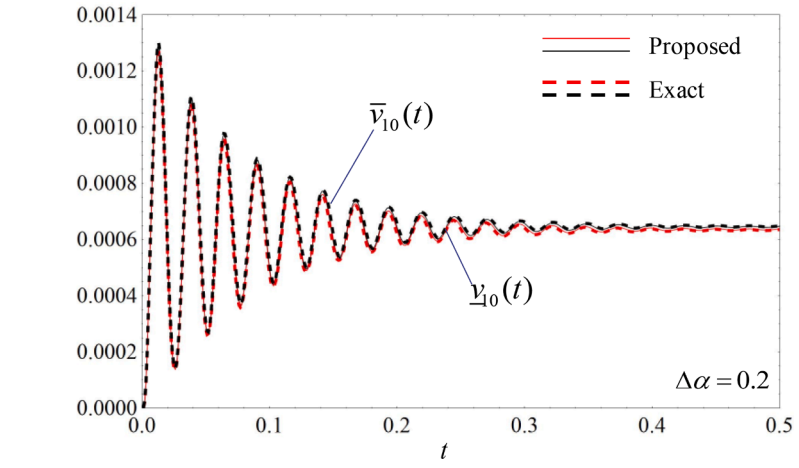

a)

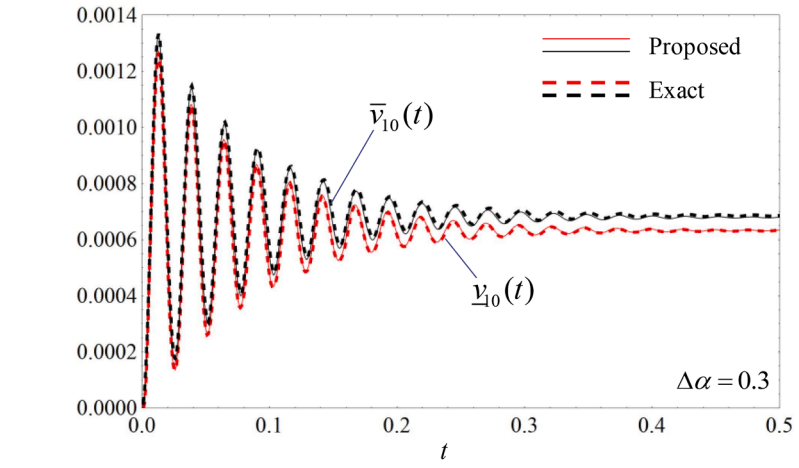

b)

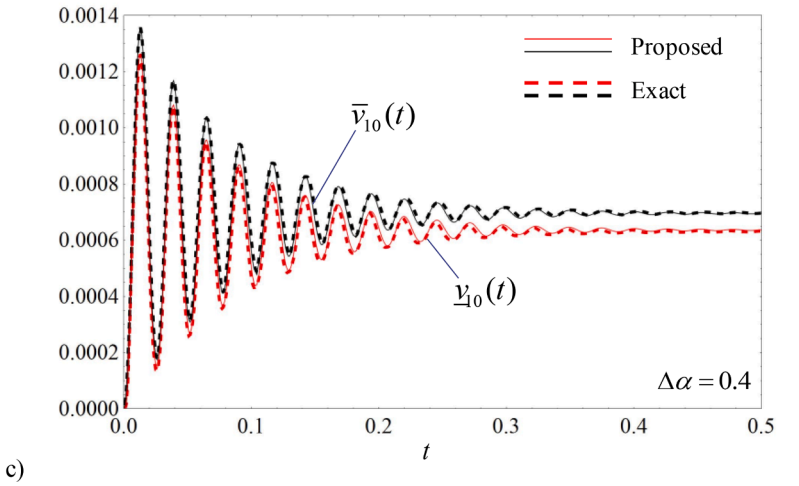

c)

Fig. 8. Time-varying lower and upper bounds of the 10-th node displacement in z-direction (in m) of the 3D multi-cracked truss structure ($i = 1,2,\ldots,13$) subjected to UnitStep function: proposed method (continuous lines) and exact solution (dotted lines) for a) $\Delta\alpha = 0.2$, b) $\Delta\alpha = 0.3$ and c) $\Delta\alpha = 0.4$.

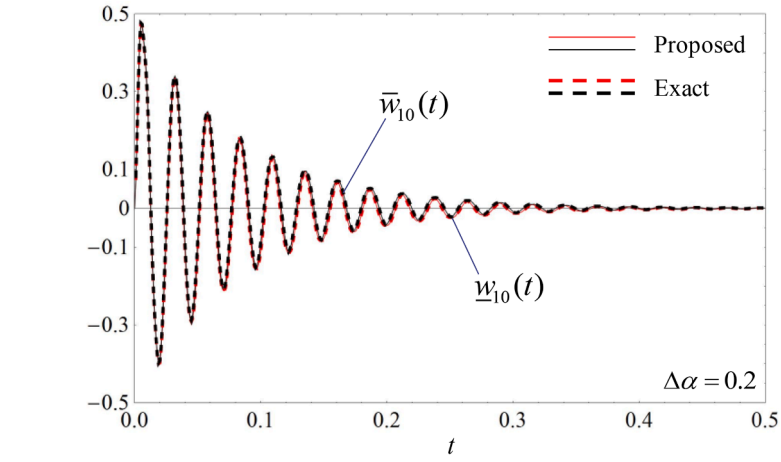

a)

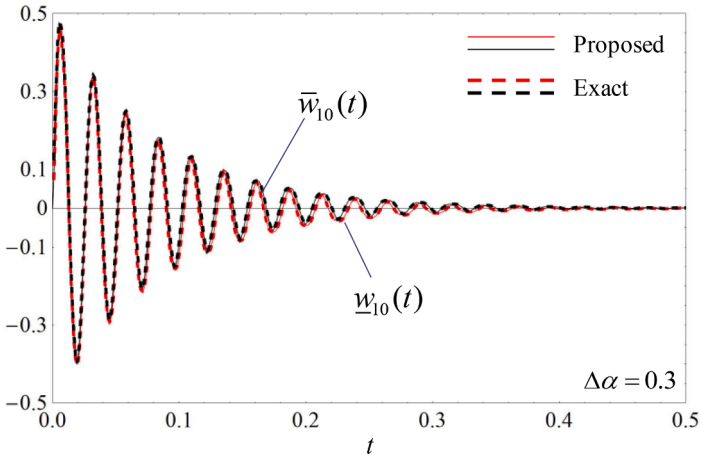

b)

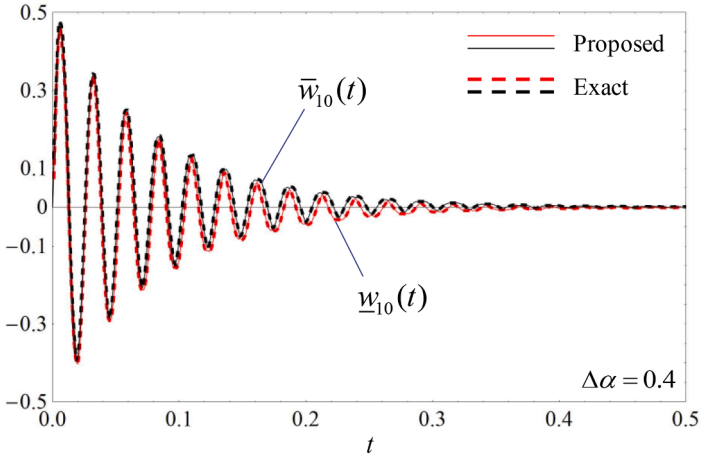

c)

Fig. 9. Time-varying lower and upper bounds of the 10-th node displacement in *y*-direction (in m) of the 3D multi-cracked truss structure ($i = 1,2,\ldots,13$) subjected to impulsive function: proposed method (continuous lines) and exact solution (dotted lines) for a) $\Delta\alpha = 0.2$, b) $\Delta\alpha = 0.3$ and c) $\Delta\alpha = 0.4$.

excellent concordance of the results shown in the graphs especially for the two levels of uncertainty $\Delta\alpha = 0.3$ and $\Delta\alpha = 0.4$, it is once again clear how the proposed procedure is highly competitive also in consideration of the substantial number of the involved uncertain parameters ($r = 13$).

The interval response of the 3D truss damaged structure has been also evaluated considering as excitation at node 9 an impulsive load with $f_{y,9}(t) = F_0\delta(t)$ where $F_0 = 150$ kN and $\delta(t)$ the Dirac delta function and selecting the interval displacement of node 10 in the load direction (y-direction) $w_{10}^I(t)$ as quantity of interest.

In this case the vectors collecting the commonest combinations read:

$$\underset{\sim}{\boldsymbol{\alpha}}_{C,w_{10}} = \left[\bar{\alpha}_{w_{10},1}\ \underline{\alpha}_{w_{10},2}\ \ \bar{\alpha}_{w_{10},3}\underline{\alpha}_{w_{10},4}\bar{\alpha}_{w_{10},5}\cdots\bar{\alpha}_{w_{10},9}\cdots\bar{\alpha}_{w_{10},13}\right]$$
$$\tilde{\boldsymbol{\alpha}}_{C,w_{10}} = \left[\underline{\alpha}_{w_{10},1}\ \ \bar{\alpha}_{w_{10},2}\ \ \underline{\alpha}_{w_{10},3}\ \ \bar{\alpha}_{w_{10},4}\underline{\alpha}_{w_{10},5}\cdots\underline{\alpha}_{w_{10},9}\cdots\underline{\alpha}_{w_{10},13}\right] \quad (45a,b)$$

where it is worth to note the vectors $\underset{\sim}{\boldsymbol{\alpha}}_{C,w_{10}}$ and $\tilde{\boldsymbol{\alpha}}_{C,w_{10}}$ collect, respectively, the upper and lower extremes of the uncertain parameters with the exception of the parameters 2 and 4.

Figs. 9a,b and c show the time varying bounds of the interval nodal displacement $w_{10}(t)$ for the three considered levels of deviation amplitude provided via the proposed procedure as well as the reference method (vertex method with $2^{r=13} = 8192$ evaluations combined with the results of the 1000 samples of the MC).

Also in this case it can be observed the excellent agreement between the results obtained by applying the two methods considering however the fact that in this case study the intervals are very narrow even for high levels of uncertainty.

It is worth to remark that the proposed method requires only two deterministic dynamic analyses despite the number r of the uncertain parameters involved proving its computational efficiency with respect to the reference methods.

4.2. *Frame-like structure with uncertain damage*

A third application concerns a steel three levels multi-cracked frame structure (see Fig. 10) subjected to horizontal forces applied at the nodes 2, 3 and 4 in the x–direction labeled as $f_{x,j}(t)$ with $j = 2,3,4$. All the beams have prismatic cross-sectional areas with $B_i = H_i = 0.1$ m ($A_i = A = 0.01$ m^2 for $i = 1,2,\ldots,15$) and same lengths $L_i = L$ with $L = 5.1$ m. Young's modulus and Poisson's ratio are fixed in $E = 2.1 \times 10^8$ kN/m^2 and $\nu = 0$, respectively. The material unit weight is $\rho = 7850$ kg/m^3. A consistent mass matrix is considered with 27 DOFs.

The damage configuration involves again $r = 10$ beams, specifically seven vertical elements (1,2,3,4,7,8 and 9) and three horizontal elements (10,14 and 15). The interval model for the crack depth $a_i^I = a_{0,i}(1 + \Delta\alpha_i e_i^I)$ is therefore adopted for $i = 1, 2, 3, 4, 7, 8, 9, 10, 14$ and 15 with nominal value $a_{0,i} = a_0 = 0.4H$ and deviation amplitudes $\Delta\alpha_i = \Delta\alpha\ \forall i$.

The mutual positions of the cracks are treated as deterministic quantities and selected as $x_{0,i} = \xi_i L_i$ with $\xi_i = 0.1\ \forall i$ (see Fig. 2). The Rayleigh damping constants $d_0 = 0.147197s^{-1}$ and $d_1 = 0.01684s$ (see Eq. (28)) have been again calculated with reference to the frame damaged configuration with the cracks depths selected to their mean value $a_{0,i} = a_0 = 0.4H\ \forall i$ and derived such that the modal damping ratio for the first and second modes of the nominal structure is $\zeta_0 = 0.05$. Results in terms of upper and lower bounds are

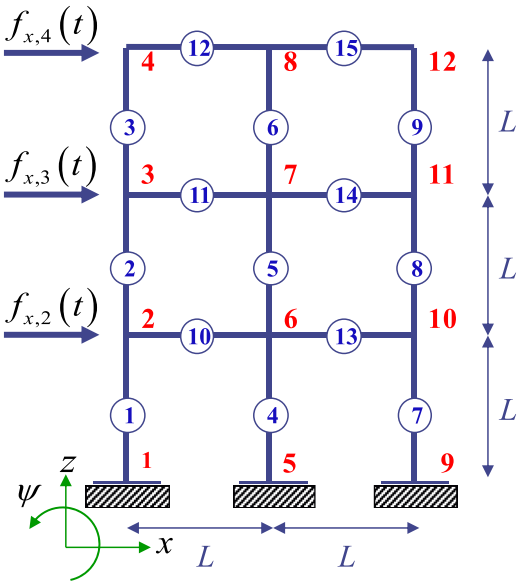

Fig. 10. 2D 27-DOFs frame structure: geometry and load condition.

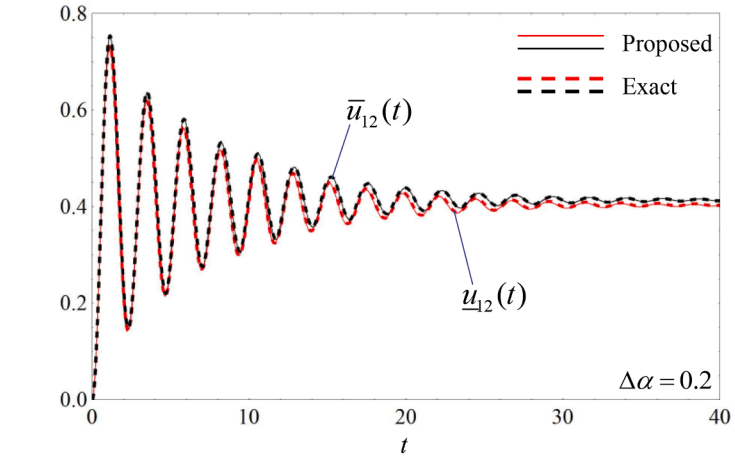

a)

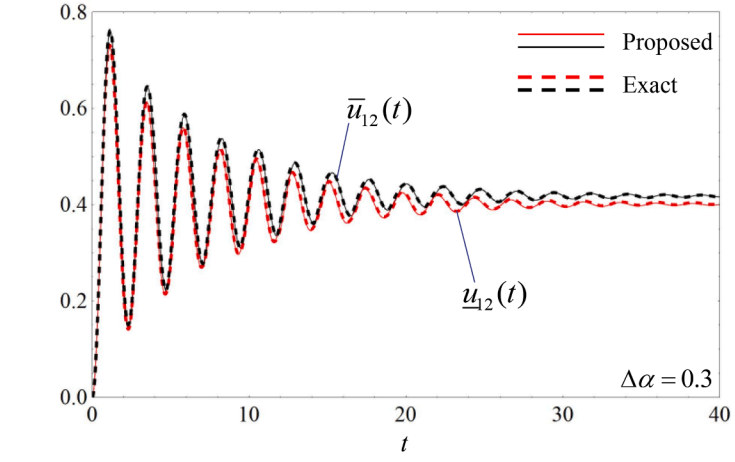

b)

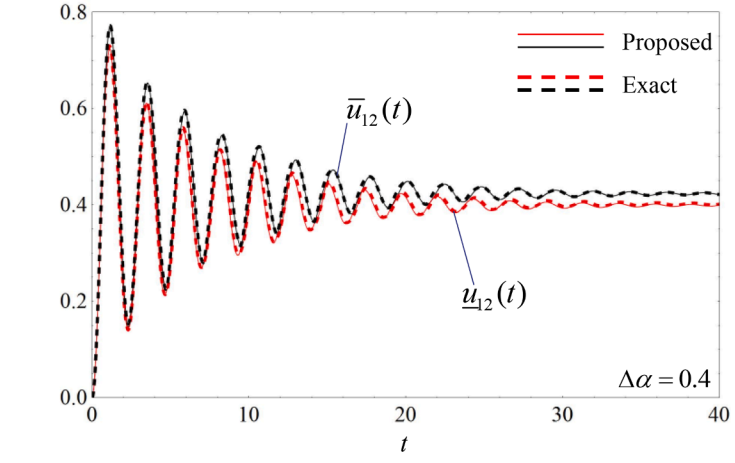

c)

Fig. 11. Time-varying lower and upper bounds of the 12-th node displacement in x-direction (in m) of the 2D multi-cracked frame structure (i = 1,2,3,4,7,8,9,10,14 and 15) subjected to UnitStep functions: proposed method (continuous lines) and exact solution (dotted lines) for a) $\Delta\alpha = 0.2$, b) $\Delta\alpha = 0.3$ and c) $\Delta\alpha = 0.4$.

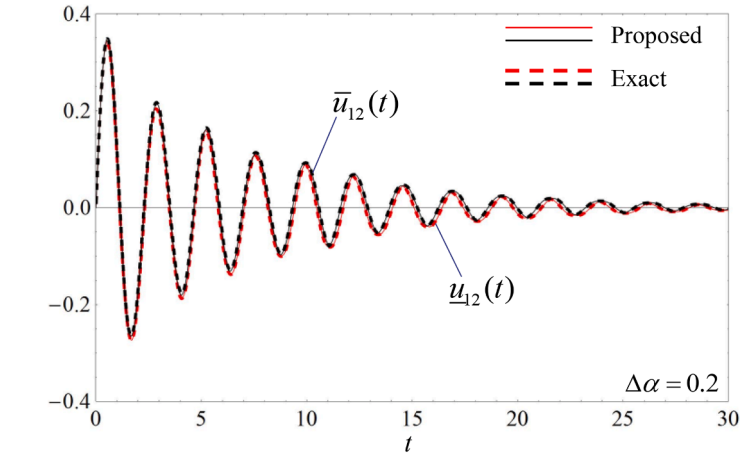

a)

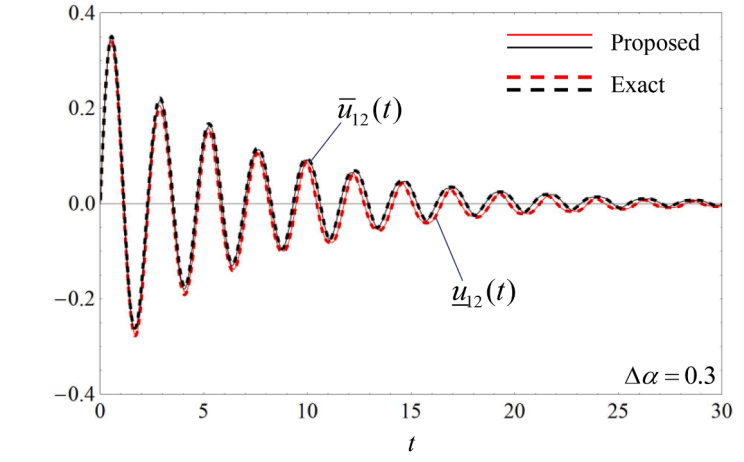

b)

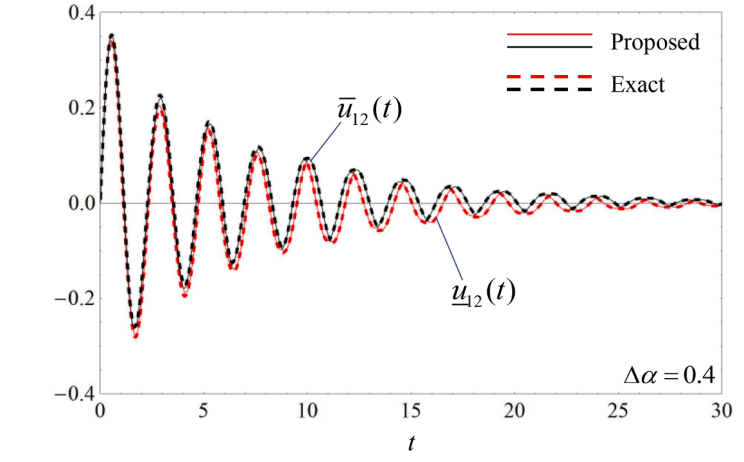

c)

Fig. 12. Time-varying lower and upper bounds of the 12-th node displacement in x-direction (in m) of the 2D multi-cracked frame structure (i = 1,2,3,4,7,8,9,10,14 and 15) subjected to impulsive functions: proposed method (continuous lines) and exact solution (dotted lines) for a) $\Delta\alpha = 0.2$, b) $\Delta\alpha = 0.3$ and c) $\Delta\alpha = 0.4$.

provided for increasing values of the deviation amplitude considering $\Delta\alpha_i = \Delta\alpha = 0.2, 0.3$ and 0.4 investigated for two cases of excitation namely $f_{xj}(t) = F_0 U(t)$ and $f_{xj}(t) = F_0\delta(t)$ with j = 2,3 and 4 where $U(t)$ and $\delta(t)$ have been previously defined. The selected response variable of interest is the 12-th node displacement in x-direction, namely $u^I_{12}(t)$.

Specifically in Fig. 11 the bounds of the response function $u^I_{12}(t)$ are reported for the first load case $f_{xj}(t) = F_0 U(t)$ with F_0 = 15 kN; Fig. 12 show the bounds of the response function $u^I_{12}(t)$ for the second load case $f_{xj}(t) = F_0\delta(t)$ with F_0 = 5 kN.

Notice that in both load cases the commonest combinations of the extremes of the uncertain parameters modeling the cracks depths for the component displacement $u_{12}(t)$ coincide with the trivial combinations:

$$\underset{\sim}{\boldsymbol{\alpha}}\, C, u_{12} = \left[\underline{\alpha}_{u_{12},1} \quad \underline{\alpha}_{u_{12},2} \quad \cdots \quad \underline{\alpha}_{u_{12},10}\right]$$
$$\tilde{\boldsymbol{\alpha}}_{C,u_{12}} = \left[\bar{\alpha}_{u_{12},1}\, \bar{\alpha}_{u_{12},2} \cdots \bar{\alpha}_{u_{12},10}\right] \tag{46a,b}$$

By observing the graphics in Figs. 11 and 12 the good accuracy of the proposed method is again confirmed: the estimated response bounds via the proposed approach almost coincide with the ones calculated via the vertex method combined with the MC ($2^{r=10}$ = 1024 deterministic dynamic analyses for the vertex method and 1000 samples for the MC).

Consider finally the multi-cracked three-dimensional frame structure shown in Fig. 13. In the computations the following data $E = 3\times 10^{10}$ N/m^2, $G = 1.8\times 10^{10}$ N/m^2 and $\nu = 0.25$ are assumed for the Young's modulus, the shear modulus and the Poisson's coefficient, respectively. The material unit weight is ρ = 2500 kg/m^3. All the beams have same lengths $L_i = L$ with L = 3 m and rectangular cross-sections $B_i \times H_i = B \times H = 0.2$ m $\times$ 0.2 m for $i = 1, 2, \ldots, 24$.

The three levels frame structure is excited by horizontal forces applied at the nodes 5, 8, 9, 12, 13 and 16 in the x–direction namely $f_{xj}(t)$ with j = 5,8,9,12,13,16. A consistent 72 $\times$ 72 mass matrix is considered in the modal analysis.

The damage scenario consists in $r = 10$ damaged beams in the vertical elements at the three levels, namely the beams 1,2,3,4 at the first level, the beams 9,10,11, 12 at the second level and the beams 18 and 20 at the third level. In the adopted interval model for the crack depth $a^I_i = a_{0,i}(1 + \Delta\alpha_i e^I_i)$ for $i = 1, 2, 3, 4, 9, 10, 11, 12, 18$ and 20, the nominal values and the deviation amplitudes are again selected as $a_{0,i} = a_0 = 0.4H$ and $\Delta\alpha_i = \Delta\alpha\ \forall i$. The non-dimensional position of the crack in the i-th beam (see Fig. 2) is fixed in ξ_i = 0.1 $\forall i$.

The Rayleigh damping constants calculated as in the previous cases with reference to the frame nominal damaged configuration take the values $d_0 = 0.84453 s^{-1}$ and $d_1 = 0.00296 s$ such that the modal damping ratio for the first and second modes of the nominal structure is ζ_0 = 0.05.

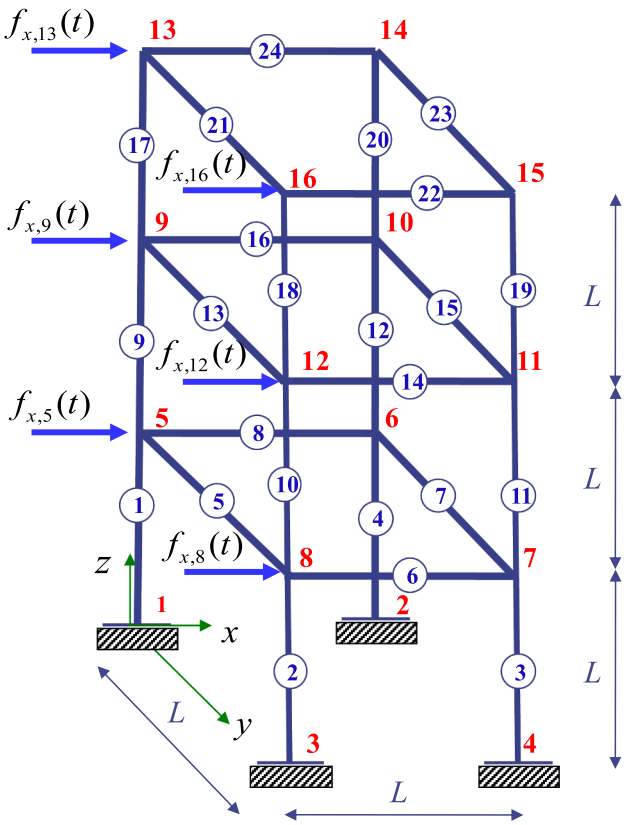

Fig. 13. 3D 72-DOFs frame structure: geometry and load condition.

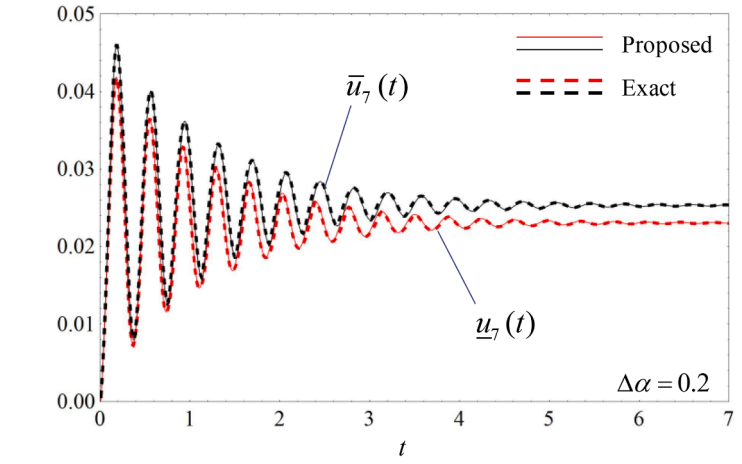

a)

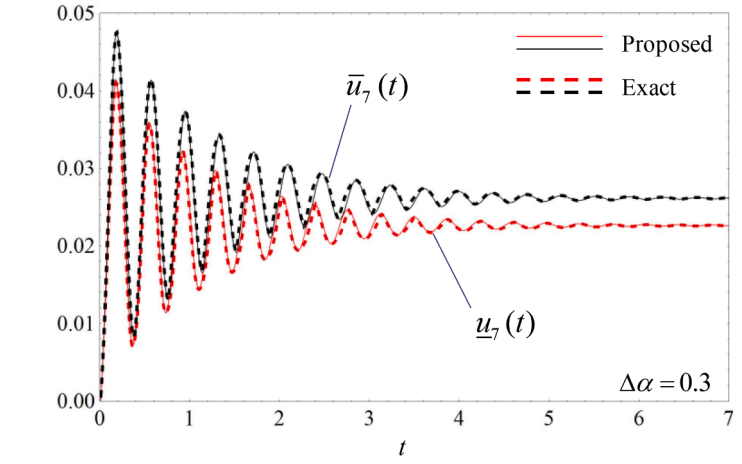

b)

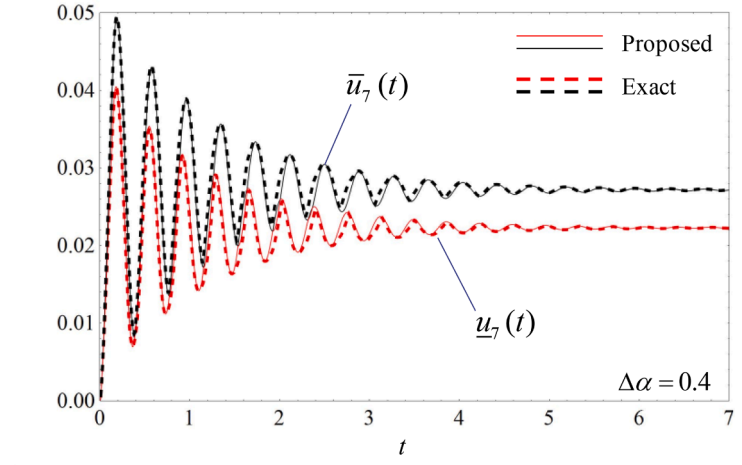

c)

Fig. 14. Time-varying lower and upper bounds of the 7-th node displacement in *x*-direction (in m) of the 3D multi-cracked frame structure (i = 1,2,3,4,9,10,11,12,18 and 20) subjected to UnitStep functions: proposed method (continuous lines) and exact solution (dotted lines) for a) $\Delta\alpha = 0.2$, b) $\Delta\alpha = 0.3$ and c) $\Delta\alpha = 0.4$.

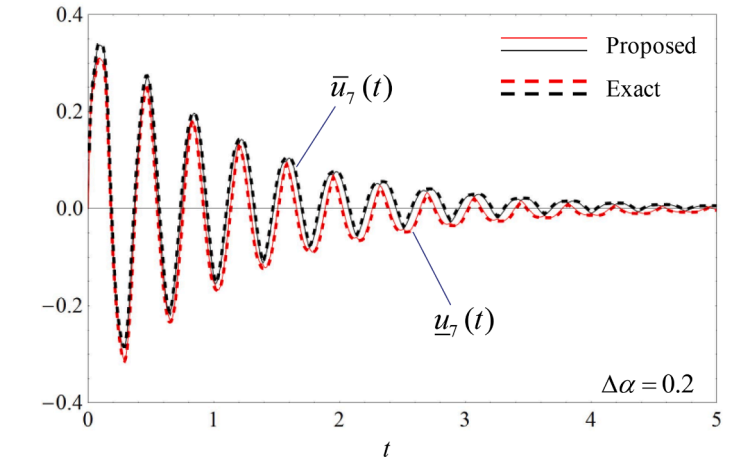

a)

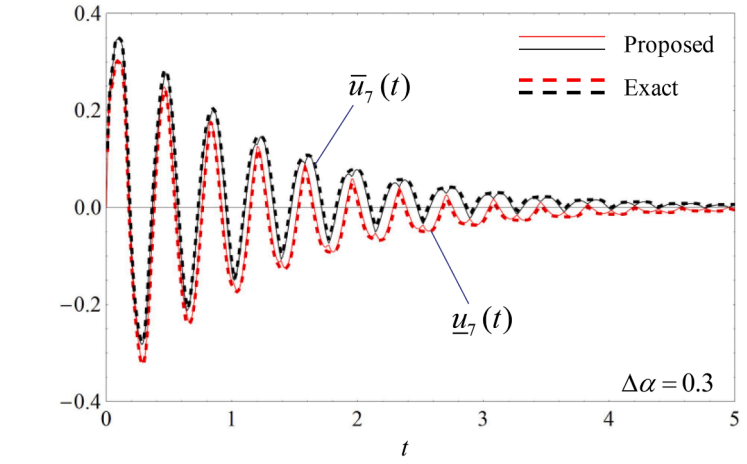

b)

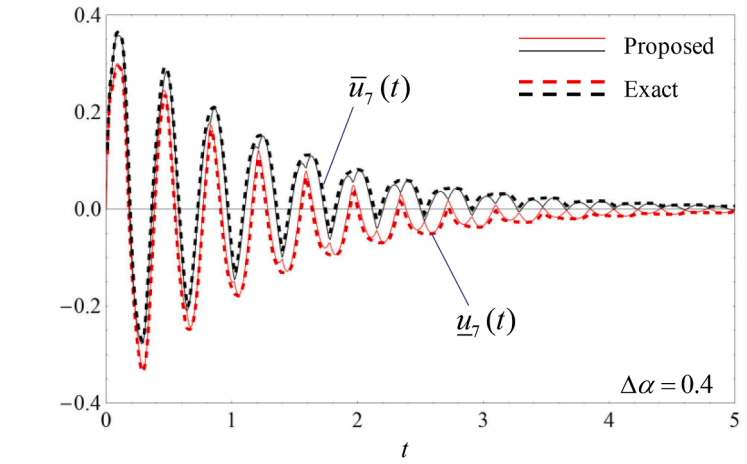

c)

Fig. 15. Time-varying lower and upper bounds of the 7-th node displacement in x-direction (in m) of the 3D multi-cracked frame structure (i = 1,2,3,4,9,10,11,12,18 and 20) subjected to impulsive functions: proposed method (continuous lines) and exact solution (dotted lines) for a) $\Delta\alpha$ = 0.2, b) $\Delta\alpha = 0.3$ and c) $\Delta\alpha$ = 0.4.

The damaged frame response for the two cases of excitation previously defined namely $f_{x,j}(t) = F_0 U(t)$ and $f_{x,j}(t) = F_0 \delta(t)$ with $j =$ 5,8,9,12,13,16 and $F_0 = 15$ kN is investigated.

The displacement of the 7-th node in x-direction, namely $u_7^I(t)$ is selected as response variable of interest and results in terms of upper and lower bounds are evaluated for increasing values of the deviation amplitude considering $\Delta\alpha_i = \Delta\alpha = 0.2, 0.3$ and 0.4, respectively in Figs. 14 and 15.

It is worth to note that for both the load cases the commonest combinations of the extremes of the uncertain parameters describing the cracks depths differ by the trivial combinations. Specifically for both the considered excitations and for the selected displacement component $u_7(t)$, the vectors $\underset{\sim}{\boldsymbol{\alpha}}\, C, u_7$ and $\widetilde{\boldsymbol{\alpha}}_{C,u_7}$ take the following forms:

$$\begin{aligned} \underset{\sim}{\boldsymbol{\alpha}}\, C, u_7 &= \left[\underline{\alpha}_{u_7,1} \quad \cdots \quad \bar{\alpha}_{u_7,10}\ \bar{\alpha}_{u_7,11}\ \underline{\alpha}_{u_7,12}\ \bar{\alpha}_{u_7,18}\ \bar{\alpha}_{u_7,20}\right] \\ \widetilde{\boldsymbol{\alpha}}_{C,u_7} &= \left[\bar{\alpha}_{u_7,1} \cdots \underline{\alpha}_{u_7,10}\ \underline{\alpha}_{u_7,11} \quad \bar{\alpha}_{u_7,12}\ \underline{\alpha}_{u_7,18} \quad \underline{\alpha}_{u_7,20}\right] \end{aligned} \tag{47a,b}$$

where the parameters $\alpha_{10}, \alpha_{11}, \alpha_{18}$ and α_{20} take their upper extreme values in $\underset{\sim}{\boldsymbol{\alpha}}\, C, u_7$ and their lower extreme values in $\widetilde{\boldsymbol{\alpha}}_{C,u_7}$.

By inspection of the graphics reported in Figs. 14 and 15, it is evident the excellent accuracy of the proposed interval solution compared with the reference one regardless the level of uncertainty considered and with a remarkable reduction of the computational cost considering only two deterministic analyses whatever the number of uncertain parameters involved.

5. Conclusions

An analytical procedure for evaluating lower and upper bounds of the dynamic response of damaged linear elastic structures in presence of multiple cracks with uncertain-but-bounded depths subjected to deterministic excitations has been presented.

The starting point of the proposed method developed in the time domain is to provide the bounds of the interval eigenvalues as solution of two appropriate deterministic eigenvalue problems without requiring any combinatorial procedure. The pseudo-static sensitivity analysis allows to identify the most common combinations of the involved uncertain parameters. The time-varying upper and lower bounds of the response were calculated for a 2D 25-bar truss structure, a 3D 26-bar truss structure and 2D and 3D three levels multi-cracked frame structures with 27-DOFs and 72-DOFs, respectively.

Effectiveness and efficiency of the present method are validated by comparing the results in terms of response bounds derived via a combinatorial procedure (vertex method) combined with the Monte Carlo (MC) method to take into account also the no monotonic behavior of the response with respect to the uncertain parameters. The excellent agreement between the two approaches also for high level of uncertainty rate revealed the accuracy of the proposed approach in dealing with these type of problems with a considerable reduction of the computational cost.

A further development of this study will concern the analysis of damaged frame structures in presence of cracks with uncertain-but-bounded positions and the effect on the structure response.

CRediT authorship contribution statement

Roberta Santoro: Conceptualization, Methodology, Software, Validation, Data curation, Writing – original draft, Writing – review & editing. **Cristina Gentilini:** Methodology, Validation, Writing – original draft.

Declaration of Competing Interest

The authors declare no conflict of interest.

Data availability

No data was used for the research described in the article.

Appendix

The local compliance contributions due to the presence of the crack in the 2D frame element (see Eq. (13) in the main text) can be evaluated by resorting to the relationship between the additional strain energy and the stress intensity factors.

The axial compliance λ_N reads:

$$\lambda_N = \frac{2(1-\nu^2)}{E} \int_0^{A_{crack}} \left(\frac{K_{IN}(a_i)}{N}\right)^2 \mathrm{d}A_{crack} \tag{A.1}$$

and coincides with the axial flexibility given in Eq. (3). The compliance λ_M related to the bending moment M, the coupled compliance

λ_{NM} related to the bending moment M and the axial force N and the compliance λ_S related to the shear force S are given by:

$$\lambda_M = \frac{2(1-\nu^2)}{E}\int_0^{A_{crack}} \left(\frac{K_{IM}(a_i)}{M}\right)^2 \mathrm{d}A_{crack} \tag{A.2}$$

$$\lambda_{NM} = \frac{2(1-\nu^2)}{E}\int_0^{A_{crack}} \left(\frac{K_{IN}(a_i)}{N}\right)\left(\frac{K_{IM}(a_i)}{M}\right) \mathrm{d}A_{crack} \tag{A.3}$$

$$\lambda_S = \frac{2(1-\nu^2)}{E}\int_0^{A_{crack}} \left(\frac{K_{II}(a_i)}{S}\right)^2 \mathrm{d}A_{crack} \tag{A.4}$$

The dependence of $\lambda_N, \lambda_M, \lambda_{NM}$ and λ_S by the crack depth a_i is omitted for the sake of brevity.

In Eqs.(A.2) and (A.3) $K_{IM}(a_i)$ is the mode I stress intensity for flexural moment:

$$K_{IM}(a_i) = \frac{6M}{B_i H_i^2}\sqrt{\pi a_i} F_M(\gamma_i) \tag{A.5}$$

while in Eq. (A.4) $K_{II}(a_i)$ is the mode II stress intensity factor for shear:

$$K_{II}(a_i) = \frac{S}{B_i\sqrt{H_i(1-a_i/H_i)}}\sqrt{\pi a_i} F_S(\gamma_i) \tag{A.6}$$

with $F_M(\gamma_i)$ and $F_S(\gamma_i)$ the correction functions given by the following expressions reported in [52]:

$$F_M(\gamma_i) = 1.12 - 1.39\gamma_i + 7.32(\gamma_i)^2 - 13.1(\gamma_i)^3 + 14(\gamma_i)^4 \tag{A.7}$$

$$F_S(\gamma_i) = 1.993\gamma_i + 4.513(\gamma_i)^2 - 9.516(\gamma_i)^3 + 4.482(\gamma_i)^4 \tag{A.8}$$

It is worth to note that the above expressions for correction functions are limited to the ratio $\gamma_i = a_i/H_i = 0.6$.

In the three-dimensional setting the local compliance coefficients appearing in Eq. (20) in the main text are again evaluated in terms of stress intensity factors via the following simplified formula:

$$\lambda_{rs} = \frac{(1-\nu^2)}{E}\frac{\partial^2}{\partial P_r \partial P_s}\left\{\int_{-B_i/2}^{B_i/2}\int_0^{a_i}\left[\left(K_{IN}+K_{IM_z}+K_{IM_y}\right)^2 + K_{IIS_z}^2 + (1+\nu)\left(K_{IIIS_y}+K_{IIIT_x}\right)^2 da_i dy\right]\right\} \tag{A.9}$$

where P_r and P_s (as well as the indices r and s) correspond to N, S_z, S_y, M_z,M_y and T_x, respectively.

The stress intensity factor K_{IN} for the axial force is

$$K_{IN} = \frac{N}{B_i H_i^{1/2}} F_{IN}(\gamma_i) \tag{A.10}$$

with

$$F_{IN}(\gamma_i) = 0.278\sqrt{\frac{(1+2\gamma_i)^3}{\gamma_i(1-\gamma_i)^3}} \tag{A.11}$$

For the bending moments M_z and M_y, the expressions for K_{IM_z} [61–63] and K_{IM_y} are:

$$K_{IM_z} = \frac{12M_z}{B_i^3 H_i^{1/2}} y F_{IM_z}(\gamma_i); \quad K_{IM_y} = \frac{6M_y}{B_i H_i^{3/2}} F_{IM_y}(\gamma_i) \tag{A.12a,b}$$

with

$$F_{IM_z}(\gamma_i) = \sqrt{\frac{\tan(\pi\gamma_i/2)}{(\pi\gamma_i/2)}}\ \frac{\sqrt{\pi\gamma_i}}{\cos(\pi\gamma_i/2)}\left(0.752 + 2.02\gamma_i + 0.37(1-\sin(\pi\gamma_i/2))^2\right) \tag{A.13a}$$

$$F_{IM_y}(\gamma_i) = \frac{0.482}{\sqrt{(1-\gamma_i)^3}} \tag{A.13b}$$

For the shear forces S_z and S_y, the stress factors K_{IIS_z} [64] and K_{IIIS_y} [65] take the following forms:

$$K_{IIS_z} = \frac{S_z}{B_i H_i^{1/2}} F_{IIS_y}(\gamma_i); \quad K_{IIIS_y} = \frac{S_y}{B_i H_i^{1/2}} F_{IIIS_y}(\gamma_i) \tag{A.14a,b}$$

with

$$F_{IIS_y}(\gamma_i) = \frac{1.2841}{\sqrt{1-\gamma_i}}; \quad F_{IIIS_y}(\gamma_i) = \sqrt{2\tan(\pi\gamma_i/2)} \tag{A.15a,b}$$

The stress factor K_{IIIT_x} related to the torque T_x is given by [63]:

$$K_{IIIT_x} = \frac{T_x}{B_i H_i^{3/2}} F_{IIIT_x}(\gamma_i) \tag{A.16}$$

with

$$F_{IIIT_x}(\gamma_i) = \frac{24\pi^3}{\pi^5\beta_i - 192\beta_i^2} \sqrt{2\tan\frac{\pi\gamma_i}{2}} \tag{A.17}$$

where $\beta_i = B_i/H_i$.

It follows that, based on Eq. (A.9), the components of interest in the flexibility matrix $\widehat{\mathbf{C}}_i^{crack}(a_i)$ can be evaluated as:

$$\lambda_N = \frac{(1-\nu^2)}{E} \frac{2}{B_i H_i} \int_0^{a_i} F_{IN}^2(a_i) da_i \tag{A.18}$$

$$\lambda_{M_z} = \frac{(1-\nu^2)}{E} \frac{24}{B_i^3 H_i} \int_0^{a_i} F_{IM_z}^2(a_i) da_i \tag{A.19}$$

$$\lambda_{M_y} = \frac{(1-\nu^2)}{E} \frac{72}{B_i H_i^3} \int_0^{a_i} F_{IM_y}^2(a_i) da_i \tag{A.20}$$

$$\lambda_{S_z} = \frac{(1-\nu^2)}{E} \frac{2}{B_i H_i} \int_0^{a_i} F_{IIS_z}^2(a_i) da_i \tag{A.21}$$

$$\lambda_{S_y} = \frac{(1-\nu^2)(1+\nu)}{E} \frac{2}{B_i H_i} \int_0^{a_i} F_{IIIS_y}^2(a_i) da_i \tag{A.22}$$

$$\lambda_{T_x} = \frac{(1-\nu^2)(1+\nu)}{E} \frac{2}{B_i H_i^3} \int_0^{a_i} F_{IIIT_x}^2(a_i) da_i \tag{A.23}$$

$$\lambda_{S_y T_x} = \frac{(1-\nu^2)(1+\nu)}{E} \frac{2}{B_i H_i^2} \int_0^{a_i} F_{IIIS_y}(a_i) F_{IIIT_x}(a_i) da_i \tag{A.24}$$

$$\lambda_{NM_y} = \frac{(1-\nu^2)}{E} \frac{12}{B_i H_i^2} \int_0^{a_i} F_{IM_y}(a_i) F_{IN}(a_i) da_i. \tag{A.25}$$

References

[1] M. Montazer, S.M. Seyedpoor, A new flexibility based damage index for damage detection of truss structures, Shock Vib. 2014 (2014), 460692, https://doi.org/10.1155/2014/460692.
[2] X. Wu, J. Xia, X. Zhu, Finding damage localizations of a planar truss using modal strain energy change, Adv. Civ. Eng. 2019 (2019), 3040682, https://doi.org/10.1155/2019/3040682.
[3] A.K. Pandey, M. Biswas, M.M. Samman, Damage detection from changes in curvature mode shapes, J. Sound Vib. 145 (1991) 321–332, https://doi.org/10.1016/0022-460X(91)90595-B.

[4] J. Ciambella, A. Pau, F. Vestroni, Modal curvature-based damage localization in weakly damaged continuous beams, Mech. Syst. Signal Process. 121 (2019) 171–182, https://doi.org/10.1016/j.ymssp.2018.11.012.
[5] E. Viola, P. Ricci, M.H. Aliabadi, Free vibration analysis of axially loaded cracked Timoshenko beam structures using the dynamic stiffness method, J. Sound Vib. 304 (2007) 124–153, https://doi.org/10.1016/j.jsv.2007.02.013.
[6] F. Wang, W.C. Cui, J.K. Paik, Residual ultimate strength of structural members with multiple crack damage, Thin-Walled Struct. 47 (12) (2009) 1439–1446, https://doi.org/10.1016/j.jsv.2007.02.013.
[7] D. Wei, Y. Liu, Z. Xiang, An analytical method for free vibration analysis of functionally graded beams with edge cracks, J. Sound Vib. 331 (7) (2012) 1686–1700, https://doi.org/10.1016/j.jsv.2011.11.020.
[8] A.R. Daneshmehr, A. Nateghi, D.J. Inman, Free vibration analysis of cracked composite beams subjected to coupled bending–torsion loads based on a first order shear deformation theory, Appl. Math. Modell. 37 (24) (2013) 10074–10091, https://doi.org/10.1016/j.apm.2013.05.062.
[9] S. Caddemi, A. Morassi, Multi-cracked Euler–Bernoulli beams: mathematical modeling and exact solutions, Int. J. Solids Struct. 50 (6) (2013) 944–956, https://doi.org/10.1016/j.ijsolstr.2012.11.018.
[10] S. Caddemi, I. Caliò, The exact explicit dynamic stiffness matrix of multi-cracked Euler-Bernoulli beam and applications to damaged frame structures, J. Sound Vib. 332 (12) (2013) 3049–3063, https://doi.org/10.1016/j.jsv.2013.01.003.
[11] K.H. Barad, D.S. Sharma, V. Vyas, Crack detection in cantilever beam by frequency based method, Procedia Eng. 51 (2013) 770–775, https://doi.org/10.1016/j.proeng.2013.01.110.
[12] A. Labib, D. Kennedy, C. Featherston, Free vibration analysis of beams and frames with multiple cracks for damage detection, J. Sound Vib. 333 (2014) 4991–5003, https://doi.org/10.1016/j.jsv.2014.05.015.
[13] S. Caddemi, I. Calio, F. Cannizzaro, The Dynamic Stiffness Matrix (DSM) of axially loaded multi-cracked frames, Mech. Res. Commun. 84 (2017) 90–97, https://doi.org/10.1016/j.mechrescom.2017.06.012.
[14] D.X. Trong, N.T. Khiem, Modal analysis of tower crane with cracks by the dynamic stiffness method, Topics in Modal Analysis & Testing, Volume 10, in: M. Mains, J. Blough (Eds.), Conference Proceedings of the Society for Experimental Mechanics Series, Cham, Springer, 2017, https://doi.org/10.1007/978-3-319-54810-4_2.
[15] B. Bozyigit, Y. Yesilce, M.A. Wahab, Free vibration and harmonic response of cracked frames using a single variable shear deformation theory, Struct. Eng. Mech. 74 (1) (2020) 33–54, https://doi.org/10.12989/sem.2020.74.1.033.
[16] C. Soize, Stochastic modeling of uncertainties in computational structural dynamics-recent theoretical advances, J. Sound Vib. 332 (10) (2013) 2379–2395, https://doi.org/10.1016/j.jsv.2011.10.010.
[17] R. Laudani, G. Falsone, Response probability density function for multi-cracked beams with uncertain amplitude and position of cracks, Appl. Math. Modell. 99 (2021) 14–26, https://doi.org/10.1016/j.apm.2021.06.005.
[18] P. Cacciola, G. Muscolino, Dynamic response of a rectangular beam with a known non-propagating crack of certain or uncertain depth, Comput. Struct. 80 (27–30) (2002) 2387–2396, https://doi.org/10.1016/S0045-7949(02)00255-9.
[19] P. Cacciola, N. Impollonia, G. Muscolino, The dynamic behaviour of a cracked beam subjected to a white noise input, in: Proceedings of the eighth international conference on The application of artificial intelligence to civil and structural engineering computing, 2001, pp. 205–206.
[20] Z. Yang, X. Su, J.F. Chen, G. Liu, Monte Carlo simulation of complex cohesive fracture in random heterogeneous quasi-brittle materials, Int. J. Solids Struct. 46 (17) (2009) 3222–3234, https://doi.org/10.1016/j.ijsolstr.2010.04.031.
[21] X. Su, Z. Yang, G. Liu, Monte Carlo simulation of complex cohesive fracture in random heterogeneous quasi-brittle materials: a 3d study, Int. J. Solids Struct. 47 (17) (2010) 2336–2345, https://doi.org/10.1016/j.ijsolstr.2010.04.031.
[22] G. Muscolino, R. Santoro, Explicit frequency response function of beams with crack of uncertain depth, Procedia Eng. 199 (2017) 1128–1133, https://doi.org/10.1016/j.proeng.2017.09.239.
[23] R. Santoro, G. Muscolino, Dynamics of beams with uncertain crack depth: stochastic versus interval analysis, Meccanica 54 (9) (2019) 1433–1449, https://doi.org/10.1007/s11012-019-01024-0.
[24] C. Gentilini, F. Ubertini, E. Viola, Probabilistic analysis of linear elastic cracked structures with uncertain damage, Probab. Eng. Mech. 20 (2005) 307–323, https://doi.org/10.1016/j.probengmech.2005.05.010, 2005.
[25] C. Gentilini, L. Nobile, Probabilistic analysis of three-dimensional beams with uncertain damage, Key Eng. Mater. 348-349 (2007) 97–100, https://doi.org/10.4028/www.scientific.net/KEM.348-349.97.
[26] R.E. Moore, Interval Analysis, Prentice-Hall, Englewood Cliffs, 1966.
[27] Z. Kulpa, A. Pownuk, I. Skalna, Analysis of linear mechanical structures with uncertainties by means of interval methods, Comput. Assist. Mech. Eng. Sci. 5 (1998) 443–477.
[28] T. Wei, F. Li, G. Meng, W. Zuo, Static response analysis of uncertain structures with large-scale unknown-but-bounded parameters, Int. J. Appl. Mech. 13 (2021), 2150004, https://doi.org/10.1142/S1758825121500046.
[29] X.-F. Ma, T.-J. Li, Dynamic analysis of uncertain structures using an interval-wave approach, Int. J. Appl. Mech. 10 (2) (2018), 1850021, https://doi.org/10.1142/S1758825118500217. Vol.
[30] R.L. Muhanna, R.L. Mullen, Uncertainty in mechanics: problems-interval-based approach, J. Eng. Mech. 127 (2001) 557–566, https://doi.org/10.1061/(ASCE)0733-9399(2001)127:6(557).
[31] D. Moens, D. Vandepitte, A survey of non-probabilistic uncertainty treatment in finite element analysis, Comput. Methods Appl. Mech. Eng. 194 (2005) 1527–1555, https://doi.org/10.1016/j.cma.2004.03.0191403.
[32] S.H. Chen, H.D. Lian, X.W. Yang, Dynamic response analysis for structures with interval parameters, Struct. Eng. Mech. 13 (2002) 299–312, https://doi.org/10.12989/sem.2002.13.3.299.
[33] Z.P. Qiu, X.J. Wang, Comparison of dynamic response of structures with uncertain-but-bounded parameters using non probabilistic interval analysis method and probabilistic approach, Int. J. Solids Struct. 40 (20) (2003) 5423–5439, https://doi.org/10.1016/S0020-7683(03)00282-8.
[34] Z. Qiu, X.J. Wang, Parameter perturbation method for dynamic response of structures with uncertain-but-bounded parameters based on interval analysis, Int. J. Solids Struct. 42 (18–19) (2005) 4958–4970, https://doi.org/10.1016/j.ijsolstr.2005.02.023.
[35] Z.P. Qiu, L. Ma, X.J. Wang, Non-probabilistic interval analysis method for dynamic response analysis of nonlinear systems with uncertainty, J. Sound Vib. 319 (2009) 531–540, https://doi.org/10.1016/j.jsv.2008.06.006.
[36] J. Wu, Y. Zhang, L. Chen, Z. Luo, A Chebyshev interval method for nonlinear dynamic systems under uncertainty, Appl. Math. Model. 37 (4) (2013) 578–4591, https://doi.org/10.1016/j.apm.2012.09.073.
[37] M. Xu, J. Du, J. Chen, C. Wang, Y. Li, An iterative dimension-wise approach to the structural analysis with interval uncertainties, Int. J. Comput. Methods 15 (06) (2018), 1850044, https://doi.org/10.1142/S0219876218500445.
[38] G. Muscolino, A. Sofi, Bounds for the stationary stochastic response of truss structures with uncertain-but-bounded parameters, Mech. Syst. Signal Process. 37 (2013) 163–181, https://doi.org/10.1016/j.ymssp.2012.06.016.
[39] G. Muscolino, R. Santoro, A. Sofi, Explicit frequency response functions of discretized structures with uncertain parameters, Comput. Struct. 133 (2014) 64–78, https://doi.org/10.1016/j.compstruc.2013.11.007.
[40] G. Muscolino, R. Santoro, A. Sofi, Explicit sensitivities of the response of discretized structures under stationary random processes, Probab. Eng. Mech. 35 (2014) 82–95, https://doi.org/10.1016/j.probengmech.2013.09.006.
[41] R. Santoro, G. Failla, G. Muscolino, Interval static analysis of multi-cracked beams with uncertain size and position of cracks, Appl. Math. Model. 86 (2020) 92–114, https://doi.org/10.1016/j.apm.2020.03.049.
[42] R. Laudani, R. Santoro (2022) An extensive comparative analysis on multi-cracked beams with uncertain damage, 233, 107594, 10.1016/j.ijmecsci.2022.107594.

[43] R. Santoro, On the interval frequency response of cracked beams with uncertain damage, in: N. Challamel, J. Kaplunov, I. Takewaki (Eds.), Modern Trends in Structural and Solid Mechanics 3: Non-Deterministic Mechanics, John Wiley & Sons Ltd, London, 2021, pp. 145–175.
[44] R. Santoro, G. Failla, An interval framework for uncertain frequency response of multi-cracked beams with application to vibration reduction via tuned mass damper, Meccanica 56 (4) (2021) 923–952, https://doi.org/10.1007/s11012-020-01290-3.
[45] L. Wang, X. Wang, H. Su, G. Lin, Reliability estimation of fatigue crack growth prediction via limited measured data, Int. J. Mech. Sci. 121 (2017) 44–57, https://doi.org/10.1016/j.ijmecsci.2016.11.020.
[46] L. Wang, J. Liang, Y.W. Yang, Y. Zheng, Time-dependent reliability assessment of fatigue crack growth modeling based on perturbation series expansions and interval mathematics, Theor. Appl. Fract. Mech. 95 (2018) 104–118, https://doi.org/10.1016/j.tafmec.2018.02.010.
[47] F. Cannizzaro, N. Impollonia, S. Caddemi, I. Caliò, Explicit dynamic response of damaged beams with application to uncertain and identification problems, J. Sound Vib. 487 (2020), 115608, https://doi.org/10.1016/j.jsv.2020.115608.
[48] G. Muscolino, R. Santoro, Dynamic response of damaged beams with uncertain crack depth, in: Proceedings of the 23rd Conference of the Italian Association of Theoretical and Applied Mechanics, 3, 2385-2397 (AIMETA 2017), Salerno, Italy, 2017. September 4-7.
[49] G. Muscolino, R. Santoro, Dynamics of multiple cracked prismatic beams with uncertain-but-bounded depths under deterministic and stochastic loads, J. Sound Vib. 443 (2019) 717–731, https://doi.org/10.1016/j.jsv.2018.11.029.
[50] G. Muscolino, A. Sofi, F. Giunta, Dynamics of structures with uncertain-but-bounded parameters via pseudo-static sensitivity analysis, Mech. Syst. Signal Process. 111 (2018) 1–22, https://doi.org/10.1016/j.ymssp.2018.02.023.
[51] H. Okamura, K. Watanabe, T. Takano, Deformation and strength of cracked member under bending moment and axial force, Eng. Fract. Mech. 7 (1975) 531–539, https://doi.org/10.1016/0013-7944(75)90053-3.
[52] T.M. Tharp, A finite element for edge-cracked beam columns, Int. J. Numer. Methods Eng. 24 (1987) 1941–1950, https://doi.org/10.1002/nme.1620241009, 1987.
[53] G. Muscolino, A. Sofi, Stochastic analysis of structures with uncertain-but-bounded parameters via improved interval analysis, Probab. Eng. Mech. 28 (2012) 152–163, https://doi.org/10.1016/j.probengmech.2011.08.011.
[54] Z. Qiu, I. Elishakoff, J.H. Starnes Jr., The bound set of possible eigenvalues of structures with uncertain but non-random parameters, Chaos Soliton Fract. 7 (11) (1996) 1854–1857, https://doi.org/10.1016/S0960-0779(96)00041-0.
[55] M. Modares, R.L. Mullen, R.L. Muhanna, Natural frequencies of a structure with bounded uncertainty. J. Eng. Mech. (ASCE), 132, (2206) 1363–1371, 10.1061/(ASCE)0733-9399(2006)132:12(1363).
[56] A. Sofi, G. Muscolino, I. Elishakoff, Natural frequencies of structures with interval parameters, J. Sound Vib. 347 (2015) 79–95, https://doi.org/10.1016/j.jsv.2015.02.037.
[57] Wolfram Research, Inc. Mathematica, Version 10.0, Champaign, IL.
[58] W. Dong, H.C. Shah, Vertex method for computing functions of fuzzy variables, Fuzzy Sets Syst. 24 (1) (1987) 65–78, https://doi.org/10.1016/0165-0114(87)90114-X.
[59] Z. Qiu, Z. Lv, The vertex solution theorem and its coupled framework for static analysis of structures with interval parameters, Int. J. Numer. Methods Eng. 112 (7) (2017) 711–736, https://doi.org/10.1002/nme.5523.
[60] Y. Li, Y.L. Xu, Increasing accuracy in the interval analysis by the improved format of interval extension based on the first order Taylor series, Mech. Syst. Signal Process. (104) (2018) 744–757, https://doi.org/10.1016/j.ymssp.2017.11.037.
[61] N. Anifantis, A.D. Dimarogonas, Stability of columns with a single crack subjected to follower and vertical loads, Int. J. Solids Struct. 19 (1983) 281–291.
[62] H. Tada, P.C. Paris, G.R. Irwin, The Stress Analysis of Cracks Handbook, Third ed., ASME Press, 2000.
[63] K. Wang, D.J. Inman, C. Farrar, Modeling and analysis of a cracked composite cantilever beam vibrating in coupled bending and torsion, J. Sound Vib. 284 (2005) 23–49.
[64] L. Nobile, Mixed mode crack initiation and direction in beams with edge crack, Theor. Appl. Fract. Mech. 33 (2000) 107–116.
[65] G.C. Sih, Handbook of Stress-Intensity Factors, Institute of Fracture and Solid Mechanics: Lehigh University, Bethlehem, 1973.